

# **Eastern Anatolia: a hot spot in a collision zone without a mantle plume**

**Mehmet Keskin**

*Istanbul University, Faculty of Engineering, Department of Geological Engineering, 34320  
Avcılar, Istanbul, Turkey. E-mail: keskin@istanbul.edu.tr*

## **Abstract**

Eastern Anatolia is one of the best examples of an active continental collision zone in the world. It comprises one of the high plateaus of the Alpine-Himalaya mountain belt with an average elevation of ~2 km above sea level. Almost two thirds of this plateau is covered by young volcanic units related to collision. They range in age from 11 Ma to Recent and have a thickness of up to 1 km in places. The collision-related volcanic province is not confined to Eastern Anatolia but extends across much of the Caucasus in the East, including Eastern Turkey, Armenia, Azerbaijan, Georgia and Southern Russia, spanning a distance of some 1000 km. The region covered by the collision-related volcanic sequences comprises a regional domal shape (~1000 km in diameter), and this unique morphology is comparable to that of the Ethiopian High Plateau except for its north-south shortened asymmetrical shape. Recent geophysical data reveal that the lithospheric mantle is exceptionally thin or absent beneath this regional dome indicating that the aforementioned dome is currently supported by the asthenospheric mantle. By these features, the Eastern Anatolia-Iranian plateau and the Lesser Caucasus region as a whole can be regarded as the site of a "melting anomaly" or "hotspot" resembling closely the setting proposed for mantle plumes. However, geologic and geochemical data provide evidence against a plume origin. Instead, the results of recent geophysical studies coupled with geologic, geochemical and experimental findings support the view that both domal uplift and extensive magma generation can be linked to the mechanical removal of a portion or the whole thickness of the mantle lithosphere, accompanied by passive upwelling of normal-temperature asthenospheric mantle to a depth as shallow as 40-50 km. Mechanical removal of the mantle lithosphere might be controlled by delamination in the north beneath the Erzurum-Kars Plateau, while it might be linked to slab-steepening and breakoff in the south. Therefore, magma generation beneath Eastern Anatolia may have been controlled by adiabatic decompression of the asthenosphere. The Eastern Anatolian example is important in showing that not only plumes but also shallow plate tectonic processes have the potential to generate regional domal structures in the Earth's lithosphere as well as large volumes of magma in continental intraplate settings.

**Keywords:** Eastern Anatolia, collision, volcanism, domal uplift, slab-breakoff, steepening, melting anomaly, hot spot, mantle plume, fertile mantle, intraplate, subduction component.

## Introduction

Orogenic belts formed by collisions between continents contain invaluable records of the geological history of the Earth and therefore have always attracted the attention of Earth scientists. The Anatolian–Iranian Plateau is one of two regions where active continent-continent collision is currently taking place, the other being the Tibetan Plateau (see Fig. 1 of Dewey et al., 1986). Therefore, Eastern Anatolia, being the Western part of the Anatolian–Iranian Plateau, can be regarded as a spectacular natural laboratory where the early stages of a continent-continent collision and their effects can be thoroughly studied.

Previous studies to date (e.g., Şengör & Kidd, 1979; Dewey et al., 1986) have shown that collision occurred between the Eurasian and Arabian continents, resulting in the formation of an extensive ( $\sim 150,000 \text{ km}^2$ ) high plateau with an average elevation of 2 km above sea level. These studies also revealed that the region reached this elevation as a block since the Serravalian ( $\sim 13\text{-}11 \text{ Ma}$ ; Gelati, 1975), when the terminal collision of Arabia with Eurasia started (Şengör & Kidd, 1979).

Volcanic activity initiated immediately after rapid block uplift of Eastern Anatolia and became widespread all over the region, producing subaerial lava flows and pyroclastic products which are very variable in their composition (i.e. from calc-alkaline to alkaline, from basalts to high silica rhyolites) and eruptive style (i.e. from Hawaiian to Plinian) (Pearce et al., 1990; Keskin et al., 1998; Yılmaz et al., 1998). The volcanic activity initiated in the north around the Erzurum-Kars Plateau with calc-alkaline lavas and migrated to the south-southeast becoming more alkaline (i.e. basically sodic alkaline) in character (Keskin, 2003). A vast volume of volcanic material was produced by this activity, covering almost two thirds of the region (i.e.  $\sim 43,000 \text{ km}^2$  in E Anatolia alone) and reaching over 1 km in thickness in some localities. Although fissure eruptions dominated the volcanic activity, there are over 20 major volcanic centres (e.g., Mt. Nemrut, Mt. Ararat, Mt. Tendürek) and numerous small ones in Eastern Anatolia, corresponding basically to central eruption sites (Fig. 1 and 2). Although it is difficult to calculate the total volume of the volcanic material produced because of variations in the thickness of the volcanic succession and erosion in the region, the estimated total volume is a minimum of  $15,000 \text{ km}^3$  in Eastern Anatolia alone (assuming an average volcanic thickness of 300–350 m). The erupted volume may represent only a small fraction of the melt generated beneath the region, because a greater proportion presumably was emplaced deeper in the crust as plutonic intrusions. Thus, there must have been enormous magma generation beneath the whole region related to the collision of Arabia with Eurasia. As a result, the Anatolian – Iranian Plateau can be regarded as one of the Earth's “hotspots” or “melting anomalies”.

The East Anatolian topographic uplift resembles the Tibetan Plateau and has been viewed as a younger version of it in many studies (e.g., Şengör & Kidd, 1979; Dewey et al., 1986; Barazangi, 1989). In these studies, the Eastern Anatolian lithosphere is thought to have doubled in thickness (to  $\sim 250\text{-}300 \text{ km}$ ) as a result of collision. However, recent geophysical studies (Gök et al., 2000, 2003; Al-Lazki et al., 2003, 2004; Piromallo and Morelli, 2003; Al-Damegh et al., 2004; Maggi and Priestly, 2005) have revealed that the mantle lithosphere is almost completely absent beneath a greater portion of the region (Figs. 3 and 4).

On the basis of these results and the geology of the region, Şengör et al. (2003) proposed that the East Anatolian high plateau is a mantle-supported, north-south shortened domal structure, whose E-W topographic profile along the  $40^\circ\text{N}$  parallel is very similar to that of the Ethiopian High Plateau (Fig. 4a). At present, it is difficult to recognise the dome in topographic maps since the topography of the region has been strongly modified by volcanoes and river drainage systems.

In what follows, I deal with a number of problems including:

- how and why the region gained its elevation and the aforementioned domal shape,
- how great volumes of collision-related magma were generated in the region, and
- what tectonic processes are responsible for both magma generation and the regional uplift.

The organization of the paper is as follows: Section I focuses on the geology of the region, Section II summarises new geophysical findings about the lithospheric structure of the region, Section III deals with the geochemical characteristics of the collision-related volcanic units, and Section IV discusses competing geodynamic models proposed for the region with an emphasis on the inherent discrepancies in each model. Sections V and VI present a discussion and conclusion.

## 1. Geology

The basement of the Anatolian – Iranian Plateau is made up of micro-continents, accreted to one another during the Late Cretaceous to Early Tertiary (Şengör, 1990). These micro-continents are separated from one another by ophiolite belts and accretionary complexes. Five different tectonic blocks are recognised in Eastern Anatolia (Fig. 1b): (1) The Eastern Rhodope-Pontide fragment in the northwest of the region (I in Fig. 1b). It underlies the south-western and north-eastern parts of the Erzurum Kars Plateau (i.e. EKP in Fig. 1b). (2) The Northwest Iranian fragment (II in Fig. 1b). The eastern part of the Erzurum-Kars Plateau (i.e. Horasan, Aladağ, Kağızman, Kars areas and Mt. Ararat) overlies this tectonic block (Keskin et al., 2006), (3) The Eastern Anatolian Accretionary Complex (EAAC) in the middle of the region located between the Aras River and the Bitlis-Pötürge Massif (III in Fig. 1b), (4) The Bitlis-Pötürge unit which is exposed along the Taurus belt (IV in Fig. 1b), and (5) Autochthonous units of the Arabian continent or foreland (V in Fig. 1b). Except for the EAAC, all the tectonic blocks correspond to the aforementioned micro-continents.

The Eastern Rhodope-Pontide unit is located in the northernmost part of the region. Its basement is represented by a metamorphic massive named the Pulus Complex (Topuz et al., 2004). The Pulus complex is composed of a heterogeneous set of granulite facies rocks, ranging from quartz-rich mesocratic gneisses to silica- and alkali-deficient, Fe-, Mg- and Al-rich melanocratic rocks (Topuz et al., 2004). A thick volcano-sedimentary arc sequence overlies this metamorphic basement. This sequence is regarded as an ensialic, south-facing magmatic arc, formed by north-dipping subduction under the Eurasian continental margin (Yılmaz et al., 1997) in a period between the Albian and Oligocene (Şengör et al., 2003).

The Northwest Iranian fragment is masked by collision-related volcanic units in Eastern Anatolia. It is exposed in Armenia around the Tsakhkuniats basement outcrop and the Hankavan-Takarly and Agveran massifs (Karapetian et al., 2001). The unit is composed of a heterogeneous rock sequence, consisting of trondhjemitic, phyllitic, albite-plagiogranitic, plagiogranite- and granite-migmatitic lithologies (Karapetian et al., 2001).

The Eastern Anatolian Accretionary Complex (EAAC) forms a 150-180 km wide, NW-SE extending belt in the middle of the region. It represents the remnant of a huge subduction-accretion complex formed on a north-dipping subduction zone located between the Rhodope-Pontide in the north and the Bitlis-Pötürge micro-continent in the south between the Late Cretaceous and Oligocene (Şengör et al., 2003). It consists of two contrasting rock units: an ophiolitic melange of Late Cretaceous age, and Paleocene to Late Oligocene flysch sequences incorporated into the ophiolitic melange as north-dipping tectonic slices. These flysch slices become younger from north to south and shallower from the Cretaceous to the Oligocene (Şengör et al., 2003). This observation is consistent with the polarity of the subduction zone thought to have created the Eastern Anatolian accretionary prism by underthrusting.

The Bitlis-Pötürge Massif is exposed in a NW-SE extending belt along the Eastern Taurus mountain range. It is regarded as the easternmost extremity of the Menderes-Taurus block. It consists of medium-to-highly metamorphosed sedimentary and igneous units.

Shallow marine deposits of Oligocene to Middle Miocene age unconformably overlie these tectonic blocks in some places (not shown in Figs. 1 and 3). Collision-related subaerial volcanic units, on the other hand, unconformably overlie both these five tectonic blocks and the aforementioned marine deposits, masking the basement units over great distances (Figs. 1a,b). These volcanic units become younger to the south/southeast (Keskin, 2003) (Fig. 1c).

## **2. Lithospheric and mantle structure beneath the region based on the results of recent geophysical studies**

Results from the Eastern Turkey Seismic Experiment project (ETSE project: Al-Lazki et al., 2003; Gök et al., 2000; 2003; Sandvol et al., 2003a; Angus et al., 2006) indicate that the mantle lithosphere is either very thin or absent beneath a considerable portion of the region between the Aras river (broadly corresponding to the southern border of the EKP) in the north and the Bitlis-Pötürge Massif in the south (Fig. 3 and 4). Barazangi et al. (2006) point out that the uppermost mantle beneath this crustal block strongly attenuates Sn waves and has one of the lowest Pn velocities on Earth (~7.6 km/s). Furthermore, crustal thicknesses obtained from receiver function studies reveal a gradual change from < 38 km in the southeast around the southern part of the Bitlis suture zone to 50 km in the north beneath the Erzurum-Kars Plateau (Fig. 4 of Zor et al., 2003; also see Çakır et al., 2000 and 2004), averaging some 45 km. This indicates that an almost normal-thickness crust overlies an extremely thin mantle lithosphere or perhaps it is almost directly underlain by the asthenosphere (see also the cross section in Fig. 3b). These results are also confirmed by the studies of Hearn & Ni (1994), Maggi et al. (2002), Sandvol and Zor (2004) and Maggi and Priestley (2005), suggesting that the temperature of the mantle significantly increased beneath this area. Moreover, high Bouguer gravity anomalies also suggest that the Moho is almost directly underlain by hot asthenospheric material beneath Eastern Anatolia (Ateş et al., 1999; Barazangi et al., 2006). This interpretation is also supported by the results of a recent magnetotelluric study conducted in the region by Türkoğlu et al. (2005 and 2006). On the basis of their geoelectric images, these researchers argue that the upper mantle beneath Eastern Anatolia has a very low resistivity and this is consistent with the presence of shallow asthenosphere beneath the region.

When all the geophysical findings are taken into consideration, a reasonable interpretation is that Eastern Anatolia's crust is hot and weak (Reilinger et al., 1997) and made up of crustal slivers which are in relative motion to one another (Angus et al., 2006). A lithospheric thickness of ~45 km is normal in extensional areas, such as Iceland, but unusual in a continental collision setting with a compressional tectonic regime. What all these findings may imply is that a huge portion of the mantle lithosphere was lost from beneath Eastern Anatolia.

Shear-wave-splitting fast polarisation directions (Fig. 3a) are quite uniform, exhibiting NE-SW orientations beneath the region (Sandvol et al., 2003b). Sandvol et al. (2003b) argue that a fundamental difference exists between the "present-day mantle flow directions" and surface deformation across the Arabian and Anatolian Plates. Therefore they suggest that the observed mantle flow directions are asthenospheric and not lithospheric. These findings are also consistent with the tomographic results and imply that most of the Eastern Anatolian mantle lithosphere has been removed.

High resolution deeper tomographic images obtained by inversion of P-wave delay times beneath the region (Piromallo and Morelli, 2003) also support the aforementioned detachment

model. Tomographic sections from Piromallo and Morelli (2003) indicate that there is a positive anomaly around the transition zone beneath Eastern Anatolia (at ~300-500 km depth; Fig. 4b and d), extending laterally to the west and merging with one beneath the Aegean Sea (Faccenna et al., 2006). These images might be interpreted as evidence for a continuous subducting slab beneath the region, extending from the Hellenic subduction zone to Central and Eastern Anatolia (Faccenna et al., 2006) where it seems to have been detached (Fig. 4b and d). Note that both beneath Eastern and Western Anatolia, slabs appear to have significantly thickened by a factor of 2 to 3. This is not unusual as it is now well understood that slabs can significantly deform during their descent into the more viscous lower mantle by means of folding and thickening (Lay, 1994; Hafkenscheid et al., 2006). Fast and steeply subducting slabs can fold and thicken by a factor of 2 to 3 (e.g. Gaherty and Hager, 1994; Christensen, 1996) while slowly subducting slabs at small angles can thicken to twice their original thickness when they enter the more viscous lower mantle (e.g. Gaherty and Hager, 1994; Becker et al., 1999).

### **3. Geochemical characteristics of the collision-related volcanic units**

One of the most striking aspects of Eastern Anatolia is the volume and compositional variability of collision-related volcanic products erupted during the Neogene and Quaternary. Over half the region is covered with young volcanic units (Figs. 1 and 3), ranging in age from 11.4 Ma to present (Figs. 1c). In this section a short description of the geochemical characteristics of the volcanic units, together with their spatial changes, are presented. Major, trace element and isotopic data from representative lava types across Eastern Anatolia are given in Table 1.

#### **3.1. Classification**

Collision-related volcanic rocks across the region span the whole compositional range from basalts to rhyolites. There is significant variation in lava chemistry in the N-S direction between the Erzurum-Kars Plateau (EKP) in the north and the Muş-Nemrut-Tendürek volcanoes in the south (Figs. 5a to 5f). Volcanic units of the Erzurum-Kars Plateau are calc-alkaline (they follow a calc-alkaline trend on the AFM diagram, which is not shown here), while those of the Muş-Nemrut-Tendürek volcanoes are alkaline to mildly alkaline in character. Lavas of the Bingöl and Süphan volcanoes display transitional chemical characteristics (Pearce et al., 1990) (Fig. 5b and e).

#### **3.2. Spatial variations in magmatism and source compositions**

##### *3.2.1. Multi-element patterns*

In order to highlight spatial variations in subduction and intraplate components in collision-related magmatism across the region, incompatible multi-element patterns normalised to N-type MORB composition are presented in Figs. 5g to 5i. The elements are arranged in the order suggested by Pearce (1983). In these diagrams, incompatibility of mobile elements increases from Sr to Ba while that of immobile elements increase from Yb to Th during lherzolite melting. Only the samples with SiO<sub>2</sub> < 60 (wt. %) have been plotted on these diagrams because fractional crystallization and crustal assimilation mask the ability of these patterns to reveal mantle sources. On these diagrams, calc-alkaline volcanic units on the EKP and Mt. Ararat display patterns typical of continental arc volcanics. They are likely to have been derived from an enriched mantle source containing a distinct subduction signature (Fig. 5g). This signature decreases to the south and diminishes around Muş-Nemrut-Tendürek volcanoes (Fig. 5i), where the lavas are alkaline and display an intraplate signature (Fig. 5h) (Pearce et al., 1990).

### 3.2.2. *Ta/Yb vs. Th/Yb plots*

On a Ta/Yb vs. Th/Yb diagram, calc-alkaline lavas of the Erzurum-Kars Plateau display a consistent displacement from the mantle metasomatism array towards higher Th/Yb ratios, forming a sub-parallel trend to the main MM (Mantle Metasomatism) array (Fig. 6a). The aforementioned displacement suggests that EKP mantle source region had a distinct subduction component. On the other hand, the presence of the sub-parallel trend to the main MM may be linked to magma chamber processes such as fractional crystallisation (FC) or AFC. It should be noted that this diagram is not suitable for differentiating between FC and AFC processes as modelled trajectories for AFC and FC processes are almost parallel. The alkaline basic lavas of the Muş-Nemrut-Tendürek volcanoes displayed a progressive shift from the MM array with increasing SiO<sub>2</sub> (Fig. 6c). Pearce et al. (1990) argued that the lavas following this trend might have been derived from an enriched source with or without a slight subduction signature and then evolved through combined assimilation-fractional crystallisation (AFC).

### 3.2.3. *Th/Ta vs. MgO and Ta plots*

In order to highlight compositional variations in magmatism across the region and their possible links with mantle source regions, Th/Ta ratios of basic samples (with MgO over 3 wt. % and SiO<sub>2</sub> ≤ 52 wt. %) have been plotted against their MgO and Ta values in Fig. 6d and e. This ratio is specifically selected as it can be used to differentiate between lavas having subduction and intraplate signatures. Note that both Th and Ta are highly incompatible during melting and with most minerals crystallizing from mafic to intermediate liquids. The Th/Ta ratio is therefore independent of partial melting and fractional crystallisation, providing that anhydrous phases (i.e. POAM) are the dominant crystallising or residual assemblages. On these two diagrams, data from lavas from northern areas (i.e. EKP and Mt. Ararat) have consistently higher Th/Ta ratios and, in general, lower Ta concentrations compared to those of the southern areas (i.e. Muş-Nemrut-Tendürek volcanoes). When interpreted with the findings from multi-element diagrams, this relationship indicates that lavas on the EKP and Mt. Ararat in the north were possibly derived from a mantle source containing a distinct subduction signature, in contrast to the lavas of the southern areas (i.e. Muş-Nemrut-Tendürek volcanoes) which were derived from a source displaying an intraplate signature with or without a slight subduction component. These observations imply that there is a north-south variation in source composition with a southward increase in intraplate signature.

## 3.3. Fractional crystallisation

Crystallization assemblages in the collision-related lavas of Eastern Anatolia also display variations across the region. Lavas in the north contain hydrous assemblages (e.g., amphibole) as well as anhydrous minerals, whereas those in the south are dominated generally by anhydrous minerals (Pearce et al., 1990). This indicates that lavas are richer in water in the north than in the south, consistent with their subduction signature. Geochemical data are also consistent with these petrographic observations: the lavas containing hydrous minerals (e.g., amphiboles) display distinct depletion in Y with increasing Rb (Low-Y series trend in Fig. 6f) in contrast to the lavas of the southern areas (i.e. Muş-Nemrut-Tendürek; High-Y trend in Fig. 6h) which contain anhydrous minerals that exhibit positive to flat gradients.

## 3.4. Summary of the geochemical findings

The geochemical evidence presented so far indicates that volcanic products in the north around the EKP and Mt. Ararat are calc-alkaline in character and likely to have been derived from a slightly enriched mantle source containing a distinct subduction signature (Figs. 5g to 5i; also see Fig. 2 of Keskin, 2003). This signature decreases to the south and diminishes around the Muş-Nemrut-Tendürek volcanoes, where the lavas are alkaline and display an

intraplate signature. Radiometric dating results published to date indicate that volcanic activity began earlier in the north than in the south, and migrated south over time (Fig. 1c). However, it should be noted that there are few good dates from the older lavas in the southern part of Eastern Anatolia. Therefore, further research is needed to confirm this trend.

The striking results of recent geophysical studies (Gök et al., 2000, 2003; Al-Lazki et al., 2003, 2004; Piromallo and Morelli, 2003; Maggi and Priestly, 2005 and Angus et al., 2006) along with the geochemical findings discussed above lead us to question the validity of geodynamic models proposed for the Eastern Anatolian Collision Zone in a number of studies reported in the literature. Therefore, prior to focusing on the issue of what process was responsible for the loss of mantle lithosphere, I first review the competing geodynamic models and their discrepancies.

#### **4. Competing geodynamic models & their discrepancies**

Ten different geodynamic models have been proposed for the genesis of collision-related magmatism beneath the Eastern Anatolian collision zone (Fig. 7). Some of the earlier studies (e.g., the tectonic escape model of McKenzie, 1972) did not address the problem of why and how huge volumes of magmas were generated beneath the region. Any geodynamic model proposed for the Eastern Anatolian collision zone should, however, answer this critical question since the topographic expression, tectonic elements and magma generation are clearly all associated with the same mechanism. Each model is now discussed thoroughly with its weaknesses and strengths.

##### **4.1. The tectonic escape of micro-plates to the east and west (McKenzie, 1972).**

Discrepancies: A close examination of the model of McKenzie (1972) reveals that it does not account entirely for the strain induced by the 2.5 cm/yr convergence of the Arabian and Eurasian plates (Dewey et al., 1986). In addition, this model cannot explain why and how huge volumes of magma were generated beneath the region and how the region was elevated to form an extensive plateau now 2 km above sea level. It also does not provide an answer to why the lithospheric mantle is absent beneath a greater portion of Eastern Anatolia (Fig. 7, Model: 1).

##### **4.2. Renewed continental subduction of the Arabian plate beneath Eastern Anatolia (Rotstein & Kafka, 1982).**

Discrepancies: this model is not supported by any seismic evidence (Fig. 7, Model: 2). There are no seismic data that suggest a currently subducting oceanic or continental lithospheric plate beneath the Bitlis-Pötürge Massif and Eastern Anatolia, attached to the Arabian plate.

##### **4.3. Detachment and northward movement of a subducting slab beneath Eastern Anatolia (Innocenti et al., 1982a,b).**

On the basis of available radiometric dating results and chemical zonation in volcanic units across the collision zone, Innocenti et al. (1982a,b) suggested that the andesitic volcanic front migrated northward by 150-200 km during the Pliocene. According to them, this is evidence for detachment of the subducted slab immediately after continental collision (Fig. 7, Model: 3). According to their model, the detached slab moved northward while it was sinking in the asthenosphere. They suggest that this movement generated progressively lower intensity magmatism from south to the north. In their view, volcanism becomes younger from south to north. In this model, calc-alkaline magmas that formed the Plio-Quaternary volcanic belt in the north were generated above the subducting slab, while the alkaline magmas

representing the Miocene volcanic belt in the south were derived from the asthenosphere upwelling through the gap behind the detached subducting slab.

Although the model of Innocenti et al. (1982a,b) is one of the earliest, it is remarkable in that the possibility of slab detachment and consequential effects on magma genesis in the Eastern Anatolian Collision Zone were envisaged 13 years earlier than the "slab-breakoff model" was proposed by Davies & von Blanckenburg (1995). The latest geodynamic model, "slab-steepening & breakoff beneath a large subduction-accretion complex", by Şengör et al. (2003) also proposes a similar slab-detachment process for magma genesis, although the slab in the model of Şengör et al. (2003) and Keskin (2003) does not move northward after breakoff but instead steepens beneath a large subduction-accretion complex until it breaks off, creating a gradually widening mantle wedge beneath the region.

Discrepancies: A more detailed study of collision-related volcanism on the Erzurum-Kars Plateau (Keskin, 1994), which comprises the northernmost part of the Eastern Anatolian volcanic province, has shown that volcanism initiated at ~ 11 Ma in the north (Keskin et al., 1998) and then migrated south over time (Keskin, 2003). These findings are the opposite of what is predicted by the model of Innocenti et al. (1982a, b).

#### **4.4. Rifting along E-W oriented Late Miocene-Pliocene basins (Tokel, 1985) possibly accompanied by decompression melting of "normal asthenosphere" due to extension (McKenzie & Bickle, 1988).**

Tokel (1985) cited data from drilling cores gathered from E-W oriented Upper Miocene-Pliocene basins in Eastern Anatolia. He argued that these basins are bounded by gravity faults and are filled with at least 2000 m of limnic and fluvial deposits intercalated with voluminous "tholeiitic" and "alkaline" volcanic products. He suggested that recent tectonics in Eastern Anatolia were dominated by an extensional stress regime. On the basis of the mathematical model of Turcotte (1983), he proposed that these depressions and the sediments deposited therein were related to a "rifting event" in the region (Fig. 7, Model: 4).

Discrepancies: The fault plane solutions of earthquakes in the region indicate that the faults are either strike slip or reverse, which is inconsistent with extension (i.e. a rift setting). A close examination of the E-W oriented basins in the region reveals that they are not rift-related but are, instead, dominantly pull-apart basins related to strike slip fault systems.

Decompression melting of normal asthenosphere as a result of regional extension (McKenzie & Bickle, 1988) requires a stretching factor of about 2.5 to generate melts in dry asthenosphere at a depth of 50 km and a temperature of around 1280°C. As is well known the region is not being stretched, so this is not a likely scenario.

#### **4.5. Continental collision and subsequent thickening of the Anatolian crust/lithosphere (Dewey et al., 1986).**

Dewey et al. (1986) argued that Eastern Anatolia owes its high elevation to a doubled (~ 300 km) lithospheric thickness (Fig. 7, Model: 5). According to them, this thickening occurred as a result of continental collision between the Arabian and Eurasian continents. They also point out that the lavas were erupted through both N-S cracks that extend into the Arabian foreland and through transcurrent pull-aparts (Fig. 7, Model: 6).

Following the model of Dewey et al. (1986), Yılmaz et al. (1987) suggested that the young volcanism in Eastern Anatolia could be linked to heating of the lower continental crust and mantle lithosphere which had been subjected to lithospheric thickening. Similarly, on the basis of their geochemical data, Koronovskiy & Demina (1996) argued that heating due to crustal thickening may explain the young volcanism of the Lesser Caucasus, adjacent to Eastern Anatolia.

Discrepancies: It is now well understood that the region would not have been isostatically elevated to  $\sim 2$  km if a 250-300 km thick and dense ( $3.2\text{-}3.3\text{ g/cm}^3$ ) mantle lithosphere had been attached to the base of a lighter ( $2.7\text{-}2.8\text{ gr/cm}^3$ ) crust (Şengör et al., 2002; Şengör et al., 2003). The model is not supported by recent tomographic data either (e.g., Al-Lazki et al., 2003; Gök et al., 2003; Maggie and Priestly, 2005) as presented in Section II.

Pearce et al. (1990) discuss the point that a 50% increase in thickness of the metasomatised mantle lithosphere lowers a significant portion of this layer to a depth below that of amphibole breakdown, forming garnet and releasing water. This may initiate localised melting but it also lowers the geotherm. When this happens, most of the metasomatised layer remains significantly below the solidus and thus does not produce magma (Pearce et al., 1990). Therefore, it is difficult to explain the huge volumes of magma generated in the region by the models of Yılmaz et al. (1987) and Koronovskiy & Demina (1996).

#### **4.6. Localized extension associated with pull-apart basins in strike-slip systems (Dewey et al., 1986; Pearce et al., 1990; Keskin et al., 1998).**

In their pioneering study, Dewey et al. (1986) highlighted the connection between the formation of pull-apart basins and volcanism (Fig. 7, Model: 6). They pointed out that there are two different neotectonic magmatic suites in the region: the nepheline-hypersthene normative alkaline basalts of mantle origin, and the silicic-to-mafic calc-alkaline suite. They suggested that both suites occur in pull-apart basins in strike slip regimes and N-S extensional fissures. They argue that the position and shape of magmatic intrusions might have been controlled by "flaking of the elastic lid" particularly beneath the pull-apart basins. In this model magma generation is linked to local extension and small-scale delamination events beneath these basins (e.g., the Erzincan, Karasu-Pasinler-Horasan and Muş basins). They also argue that rapid lithospheric stretching and small-scale delamination beneath pull-apart basins can generate melting in the mantle.

Although Pearce et al. (1990) consider delamination to be the dominant process that caused voluminous magma generation beneath the region, they also argue that it might have been accompanied by other stretching mechanisms, such as the creation of pull-apart basins. They also suggested that deviatoric stress perpendicular to the principal direction of compression might also have some effect.

Keskin et al. (1998) emphasise the role of strike-slip faulting in pull-apart basins in focussing magmas on the Erzurum-Kars Plateau, north of the region. They point out that, compared to nearby areas, a much thicker (2-4 km) sequence of volcanic/volcano-clastic rocks was deposited in these gradually subsiding basins. However, it is not clear whether these faults simply provide fractures that enable magma to reach the surface or whether the associated localised extension in pull-apart basins also encourages melting in the mantle. More recently Cooper et al. (2002) suggested a similar model for the origin of mafic magmas beneath northwestern Tibet and argued that these lavas might have been created by mantle upwelling beneath the releasing bends of the strike-slip fault systems.

Discrepancies: Collision-related volcanic units are not confined to pull-apart basins. Instead, they cover a much greater area away from these basins. Therefore, it is doubtful that a pull-apart model can explain the genesis of all the collision-related magmatism in the region.

#### **4.7. Hot spot activity related to a mantle plume (discussed by Pearce et al., 1990 and proposed as a model by Ershov and Nikishin, 2004).**

The possibility of plume-related "hot spot" activity in Eastern Anatolia was first discussed by Pearce et al. (1990) and recently proposed as a model for the Anatolian-Iranian Plateau by Ershov and Nikishin (2004) (see Fig. 7, Model: 7). Pearce et al. (1990) point out the remarkable correlation between topographic and volcanic expressions in Eastern Anatolia.

The Eastern Anatolia topographic uplift has an asymmetric (i.e. deformed) dome shape (Şengör et al., 2003) whose long-axis aligns approximately E-W. The overall volcanic expression is also asymmetric, extending about 300 km in the direction of compression but 900 km perpendicular to it (Pearce et al., 1990). This remarkable correlation between the topography and volcanic expression brings into question whether there is a mantle plume beneath the Eastern Anatolia Collision Zone. Note a plume is defined here as a passive, diapiric upwelling of material from the deep mantle.

As previously stated, Şengör et al. (2003) argued that the cause of the domal uplift in both Eastern Anatolia and the Ethiopian High Plateau was the same: hot, rising asthenosphere beneath crust bereft of underlying mantle lithosphere. Although domal uplift related to a mantle plume is expected to have a symmetrical shape, in theory, it may acquire an asymmetrical shape in a collision setting due to compression. However, there is no modern or ancient example anywhere in the world of a plume-related dome structure deformed by shortening in a collision zone.

Ershov and Nikishin (2004) propose that volcanism on the Eastern Anatolian plateau and Armenia can be explained by extraordinary lateral spreading of the African “superplume”. They argue that the lithosphere is relatively thin along a S-N line extending from Afar to Anatolia due to a previous orogenic collapse event that occurred at around 550 Ma (i.e. an-African–Mozambique–Arabian orogen). In their view, lateral asthenospheric mantle flow coming from the African superplume flowed along a lithospheric channel and moved to the north, resulting in the migration of the volcanism and uplift along a N-S belt. They claim that volcanism migrates to the north from Kenya (37-45 Ma), to Syria (9-13 Ma), Anatolia (11 Ma) and finally Armenia (11-2.8 Ma) (see Figs. 2 and 3 of Ershov and Nikishin, 2004). They argue that a slab-breakoff event took place around 11 Ma along the Eastern Taurus belt and produced a slab-window through which the asthenospheric flow passed and reached the Anatolian and Armenian plateaus, creating uplift and extensive volcanism in the north.

Discrepancies: Most domal structures though to be formed by plumes are expected to contain fault systems and dyke swarms distributed radially. Such faults and dykes are absent in Eastern Anatolia. Fault plane solutions of earthquakes imply that the faults are either transform or reverse; not normal as would be expected in a plume-related domal structure. A plume model cannot explain why volcanic units contain a distinct subduction component in the north of Eastern Anatolia, and why this component gradually diminishes to the south. It is also difficult to explain by a plume model why volcanism migrated south with time, and why there is a gradual change in magma chemistry from calc-alkaline in the north to alkaline in the south. As pointed out by Pearce et al. (1990), volcanic activity over the last 6 Myr displays a temporal change from more regional-scale activity to localised activity on a set of aligned central volcanoes. Such an evolutionary sequence is the reverse of what is expected in plume-related volcanic activity. On the basis of these discrepancies, I argue that a plume is not a viable model for the Eastern Anatolian Collision Zone. However, it should be noted that some of the characteristic features discussed above may not be observed in every hotspot setting as in the case of Ethiopian rift reported by Peccerillo et al. (2003).

Lateral spreading of the African superplume over great distances through a N-S channel along a previously thinned lithospheric domain (Ershov and Nikishin, 2004) does not seem to be a viable model because not only does it involve an unrealistic scenario that involves the lateral migration of plume-related material for unreasonably great distances, but also both magma generation and domal uplift can theoretically be generated by slab-breakoff alone without need for a plume-related hot mantle flow as will be thoroughly covered in the discussion section.

#### **4.8. Delamination of mantle lithosphere beneath the region (proposed by Pearce et al., 1990; refined by Keskin et al., 1998).**

Delamination of a thickened thermal boundary layer is plausible since it is colder and thus denser than the underlying asthenosphere (Fig. 7, Model: 8). It could therefore be convectively replaced by asthenosphere (Houseman et al., 1981; England and Houseman, 1988). Platt and England (1993) argue that magmatism in mountain belts could be evidence of delamination of the lower part of the thickened mantle lithosphere. Figs. 8a and 8b illustrate the delamination model in a 3D block diagram for Eastern Anatolia (modified from Keskin, 1994). This process is likely to be an effective mechanism for generating large volumes of collision-related magma across the region, since asthenosphere is brought into close contact with a thickened layer of metasomatised lithosphere (Pearce et al., 1990). When delamination occurs, it causes a perturbation in what is left of the mantle lithosphere, raising some parts of it above its solidus. While sinking into the asthenosphere, the delaminated block of the mantle lithosphere may release water that also promotes melting (Elkins-Tanton, 2004). These two mechanisms play an important role in the generation of extensive partial melting in the mantle, and can produce widespread volcanism in the region (Fig. 8b).

Pearce et al. (1990) argue that the region is characterised by a set of mantle domains that run parallel to the collision zone. They suggest that each domain has yielded magmas of particular composition since the beginning of the magmatism in the region. This may also be regarded as supporting evidence for the delamination model.

On the basis of estimates of the active slip rates, total convergence and timing of collision-related deformation across the Arabia-Eurasia collision zone, coupled with the interpretation of a cross-section produced by the National Iranian Oil Company (1977), Allen et al. (2004) suggest that the collision-related magmatism, which initiated at ~ 11 Ma (Keskin et al., 1998) pre-dates shortening of the crust in the region. Therefore, they argue, a sudden and regional delamination event is not a viable model. However, results obtained from three independent seismic studies presented in Section II reveal that most of the Eastern Anatolian Collision Zone is devoid of a mantle lithosphere. Therefore, geophysical findings support a major lithospheric detachment beneath the region and contradict the interpretation of Allen et al. (2004).

Discrepancies: As discussed in Section II, new geophysical data indicate that there appears to be no lithospheric mantle over a greater portion of the area beneath the region. If this is the case, then the delamination must have been a shallow event involving the whole lithospheric mantle and perhaps even the lower crust (e.g. as exemplified by Lustrino, 2005). In the absence of metasomatised lithospheric mantle, the source region of the volcanism would, then, be asthenospheric mantle as all lavas across Eastern Anatolia have mantle signatures.

Because the basement of a great portion of Eastern Anatolia between the Aras River in the north and Lake Van in the south is represented by a subduction-accretion complex (i.e. EAAC in Figs. 1b), and such large subduction-accretion complexes are devoid of lithospheric roots as they are produced on, and supported by subducting oceanic slabs, the delamination model cannot be a viable one for the areas covered by the EAAC as discussed in Section 4.10.

#### **4.9. Inflow of lower crust driven by the isostatic response to denudation and sedimentation in surrounding areas (Mitchell & Westaway, 1999).**

On the basis of their study of Neogene-Quaternary uplift and magmatism in the Greater Caucasus, Mitchell & Westaway (1999) proposed an alternative model to explain the formation of high mountain ranges and plateaus such as the Greater and Lesser Caucasus

including the Armenian highlands adjacent to North-eastern Anatolia. They argue that the rate and spatial scale of uplift of the Caucasus are too great to be the result of plate convergence alone, and therefore some other processes must have been operational.

Mitchell & Westaway (1999) argue that when crustal material is hotter than 300°C, it starts to behave in a ductile way, deforming plastically. The depth at which this temperature is reached (~ 15-20 km) broadly corresponds to the boundary between the plastic lower crust and the brittle upper crust. In the lower crust, the direction of movement (i.e. direction of flow) is determined by pressure gradients caused by lateral variations in the depth of the base of the brittle layer (Mitchell & Westaway, 1999). In this model, most of the crustal deformation occurs in the lower crust in an atectonic fashion (e.g. Kaufman & Royden, 1994).

The model of Mitchell & Westaway (1999) is dramatically different from the other competing models in that crustal thickening is not caused directly by plate motions. Their model involves lateral inflow of ductile lower crust, driven by the isostatic response to denudation of a mountain range and sedimentation in its surroundings. According to these authors, the start of uplift of the Caucasus and surrounding areas relates to changes in environmental conditions in the Late Miocene. The Messinian drawdown of sea-level in the Mediterranean region resulted in complete desiccation of the Black Sea (Giavanoli, 1979). This was accompanied by drawdown of Caspian Sea level. Not only did this result in an increase in subaerial relief, but also in an increase in the denudation rate of the Greater Caucasus. Coupled denudation and sedimentation (Fig. 7, Model: 9) caused lateral inflow into the lower crust towards the base of the mountain range, resulting in uplift along the length of the Caucasus.

Mitchell & Westaway (1999) suggest that atectonic thickening of the continental crust keeping mantle lithosphere thickness constant would raise the temperature in the mantle lithosphere, resulting in melting and magma generation as suggested by Koronovskiy & Demina (1996). They argue that this process was responsible for both uplift and volcanism in the Lesser Caucasus, including Armenia, adjacent to Eastern Anatolia. They also suggest that this process could be a viable model for Eastern Anatolia (Rob Westaway, personal communication, 2002).

Discrepancies: In this model, thickening occurs only in the lower crust by means of lateral flow driven by plastic deformation (Fig. 7, Model: 9). In such a case, a normal thickness of lithospheric mantle is still expected beneath the thickened crust, as there is no reason why it should have been detached from the base of the crust or along the thermal boundary layer. However, there is strong seismic evidence for a major lithospheric detachment event beneath the region (see Section II). Moreover, as previously discussed, an increase in the thickness of the lithosphere is not able to generate a significant amount of magma, as it remains well below its solidus (Pearce et al., 1990). Therefore, the model of Mitchell & Westaway (1999) is not consistent with new geophysical findings and fails to explain the volume and variability of magmatic products across the region.

#### **4.10. Slab-steepening and breakoff beneath a subduction-accretion complex (proposed by Şengör et al., 2003; supported by Keskin, 2003).**

Şengör et al. (2003) pointed out that areas with no mantle lithosphere, located in the south of the EKP, coincide broadly with the East Anatolian Accretionary Complex (EAAC) of late Cretaceous to earliest Oligocene age. The basement of a great portion of Eastern Anatolia between the Aras River in the north and Lake Van in the south is represented by the EAAC (Figs. 1b). Following the subduction-accretion hypothesis (Şengör & Yılmaz, 1981; Şengör & Natal'in, 1996a), Şengör et al. (2003) argue that the EAAC can be regarded as a remnant of a large accretionary prism located between the Pontides and the Bitlis-Pötürge Massif, having formed on northward-subducting oceanic lithosphere. In contrast to continental blocks, large

subduction-accretion complexes do not have their own lithospheric roots, as they are produced on, and supported by, subducting oceanic slabs. In theory, this area should have been underlain by a subducting slab, not by sub-continental mantle lithosphere, before the lithospheric detachment event. Therefore, what took place beneath the region could not have been a shallow lithospheric delamination event (Şengör et al., 2003; Keskin, 2003). As tomography provides no evidence for a mantle lid beneath the region, then the underlying slab must have detached and sunk into the asthenosphere possibly immediately prior to the domal uplift of the region at ~ 11-13 Ma. Therefore, this event can be ascribed to the past breakoff of the inferred slab beneath the EAAC (Figs. 7, Model: 10). Deep tomographic sections of Piromallo and Morelli (2003), illustrating a detached slab around 300-500 km depth (Fig. 4b and d) support this interpretation.

A modified version of the slab-breakoff model was recently proposed by Barazangi et al. (2006). The authors argue that there were two northward subducting slabs in close proximity beneath the region during the Late Miocene: the one in the north subducted beneath the EAAC, the other shallowly descended beneath the Bitlis-Pötürge Massif i.e., the oceanic segment of the Arabian lithosphere. In their view, the slab in the south (i.e. the Arabian slab) beneath the Bitlis-Pötürge Massif broke off around 11 Ma, producing widespread volcanism and resulting in a regional uplift across the Eastern Anatolian plateau.

There seems to be a discrepancy in this model. Although I agree with the possibility of Arabian slab breakoff in the south, the timing of this event does not seem to be reasonable. Arabian slab breakoff beneath the Bitlis-Pötürge Massif about 11 Ma would have generated a widespread volcanism on the Massif because it would have opened up a slab-window right below this continental sliver (See Fig. Fig. 7: the last model; also see 7c in Barazangi et al., 2006). However, such young volcanism ( $\leq 11$  Ma) does not exist anywhere along the Bitlis-Pötürge massif, and this contradicts the model of Barazangi et al. (2006). Therefore, Arabian slab breakoff in the south might be an older event (e.g. Eocene-Oligocene).

There appear to be inconsistencies in all models except for the delamination and slab-steepening & breakoff models. In view of these arguments, a model involving steepening and breakoff of a subducting slab beneath a huge subduction-accretion complex can explain better the geodynamic evolution of the Eastern Anatolian Collision Zone (Şengör et al., 2003) and widespread magmatism (Keskin, 2003) (Fig. 7, Model: 10) as will be discussed in the next section.

## 5. Discussion

Keskin (2003) showed that volcanic activity in Eastern Anatolia began earlier in the north (i.e. almost coeval with the rapid regional block uplift at ~ 11–13 Ma) than in the south, migrating south with time (Fig. 1c). This migration was accompanied by significant variation in lava chemistry in the N-S direction between the EKP in the north and the Muş-Nemrut-Tendürek volcanoes in the south (Figs. 5 and 6). As presented earlier in Section 3, volcanic products erupted in the north around the EKP are calc-alkaline in character with a distinct subduction signature in contrast to the ones in the south around the Muş-Nemrut-Tendürek volcanoes which are alkaline with an intraplate signature (Pearce et al., 1990). The volcanic units of the Bingöl and Süphan volcanoes display transitional chemical characteristics (Fig. 5).

Şengör et al. (2003) and Keskin (2003) pointed out that these spatial and temporal variations in magma genesis, coupled with the uplift history of the region, can be explained by a model involving steepening of a northward subducting slab beneath a large subduction-accretion complex, namely the EAAC, followed by breakoff at around 10-11 Ma. Keskin (2003) points out that the slab, whose subduction was generating the Pontide arc in the north,

was not attached to the Arabian plate. Instead, it was possibly attached to the Bitlis-Pötürge block before breakoff (Fig. 9). The oceanic realm between the Bitlis-Pötürge Massif and the Arabian plate had been closed much earlier (i.e. in the Late Eocene: Şengör et al., 2003). Therefore, it is not surprising that researchers failed to reach a consensus regarding timing of the collision event in the region.

According to Şengör et al. (2003), the oceanic realm between the Pontides and the Bitlis-Pötürge Massif was completely closed in the Oligocene (see Fig. 3 of Şengör et al., 2003 and Fig. 3c of Keskin, 2003). After a period between the Oligocene and Serravalian, during which the EAAC was shortened and thus thickened over the slab, the hidden subduction possibly stopped (Fig. 10a; see Fig. 3d of Keskin, 2003). As a result, being left unsupported by subduction, the dense oceanic lithospheric slab may have steepened and finally detached from the EAAC (Şengör et al., 2003), opening out an asthenospheric mantle wedge, gradually widening to the south (Figs. 9 and 10b,c). This possibly created suction on the asthenosphere, generating mantle flow to the south (Figs. 9b and 10b,c).

Emplacement of the asthenospheric mantle with a subduction component (especially water) and a potential temperature of 1280°C at shallow depths (~ 40-50 km) beneath the EAAC would have generated extensive adiabatic decompression melting in the mantle wedge (Keskin, 2003). Also, it probably generated regional block uplift, producing the regional dome-like structure (Şengör et al., 2003) (Figs. 9b and 10c).

The presence of such asthenospheric flow, related to opening out an asthenospheric mantle wedge, may provide an answer to the question of why the volcanic activity initiated much earlier in the north on the EKP and migrated to the south over time. Similarly, it explains better why the volcanic products are calc-alkaline with a distinct subduction signature in the north (Figs. 9b and 10b,c).

Deep tomographic images of the region (Piromallo and Morelli, 2003) provide evidence for a lithospheric mantle fragment, possibly a slab, at a depth of around 300-500 km, currently sinking into the asthenosphere beneath Eastern Anatolia (Fig. 4b and d). What this may indicate is that the detachment of the oceanic lithosphere of the Arabian plate took place in the past, perhaps millions of years ago (i.e. ~11 Ma; Figs. 9 and 10c).

I suggest that the mantle source region owed its exceptional fertility either to a subduction component inherited from a previous subduction event (i.e. the subduction beneath the Pontides during the Eocene and Oligocene), to the oceanic crustal material previously subducted beneath the region (see inferred detached lithospheric fragments in Fig 4d), or to a combination of both. A process similar to the latter has recently been proposed by a number of researchers (e.g., Gasparik, 1997; Anderson, 2000; 2004a; this volume; Balyshev and Ivanov, 2001; Ivanov, 2003; Foulger et al., 2005) to explain low velocity anomalies in the mantle as well as the genesis of magmatism in exceptionally fertile mantle domains (e.g., the Icelandic hot spot; Foulger et al., 2005). Alternatively, delaminated lithospheric blocks beneath the northern part of the region (i.e. the Erzurum-Kars Plateau), where a lithospheric mantle root is thin but still exists, might have contributed to the magma generation by dewatering themselves as they sank (a process described by Elkins-Tanton, 2004). Although not clear, such detached blocks seem to exist in the mantle wedge beneath the Erzurum-Kars Plateau in the tomographic images of Piromallo and Morelli (2003) (Fig. 4d). As pointed out by Anderson (2004a,b), melting anomalies can result from fertile patches or regions of shallow mantle with low melting point, and this seems to be the case for Eastern Anatolia.

Recent experimental studies by Regard et al. (2005, 2006) and Faccenna et al. (2006) and deep tomographic images of Piromallo and Morelli (2003) support the slab-breakoff model for Eastern Anatolia. Faccenna et al. (2006) argue that deep deformation of the Bitlis-Hellenic slab by means of slab breakoff beneath Eastern Anatolia and its lateral effect in the western part of the subduction system (i.e. Hellenic arc and Aegean region) in the form of slab-

rollback might be responsible for the fundamental plate-tectonic reorganisation during the Late Miocene – Early Pliocene period in Anatolia and the surrounding areas. They claim that the aforementioned reorganisation in the slab geometry beneath Eastern Mediterranean region might have created the North and South Anatolian Transform Fault systems that currently control the dynamics of the whole Neotectonic system. Results of a recent GPS study by Reilinger et al. (2006) support the interpretation of Faccenna et al. (2006) and further indicate that slab rollback, possibly driven by slab breakoff in the east, might be responsible for both westward motion of Anatolia and counterclockwise rotation of the whole of Arabia and Anatolia.

In order to understand how a wide hot orogen with a relatively thin lithosphere (e.g. Tibetan and Anatolian-Iranian plateaus) is deformed during collision, Cruden et al. (2006) constructed a set of analogue vice models and conducted two dimensional numerical experiments. Results of their experimental studies revealed that ductile lower crust and mantle in the weak lithosphere could flow laterally parallel to the orogen, producing upright folding in the upper crust and decoupled horizontal strain in the lower crust. One of their experiments (Experiment #32) produced an impressively similar result to the deformation style of the Eastern Anatolian-Iranian Plateau (i.e. in terms of its fold and fault geometry), supporting the presence of an exceptionally thin lithosphere over a hot and relatively buoyant mantle beneath Eastern Anatolia.

In another recent study, Hafkenscheid et al. (2006) investigated the Mesozoic-Cenozoic subduction history of the Tethyan region by integrating independent information from mantle tomography (Bijwaard et al., 1998) and tectonic reconstructions. Their aim was to test three different tectonic reconstructions proposed by Dercourt et al. (1993), Şengör and Natal'in (1996b), Norton (1999) and Stampfli and Borel (2002, 2004) by comparing the predicted thermal signature of the subducted lithosphere to the tomographic mantle structure underneath the Tethyan region. They argue that the sizes and positions of their analyzed tomographic volumes can be best explained by a slab breakoff event around 12 Ma beneath Eastern Anatolia and 30 Ma further in the east (i.e. the northern Zagros suture zone). They point out that the slab breakoff might have initiated ~30 Ma beneath the Northern Zagros suture zone and then propagated both eastward and westward along the suture zone, reaching Eastern Anatolia around 12 Ma.

An interesting feature of the Eastern Anatolia collision zone is the gradual weakening of collision-related volcanism across the region. On the basis of their numerical model, Gerbi et al. (2006) argue that when wholesale lithospheric delamination occurs, the result would be dramatic heating of the lower crust by the asthenosphere. This process causes low-pressure metamorphism while the hot asthenosphere cools, turning into the lithospheric mantle beneath the crust (Fig. 10c). Thickening of the lithosphere by reformation of the lithospheric mantle in this way (i.e. via conductive cooling of the asthenospheric mantle) might have been an important process for the weakening of volcanic activity during the course of time across Eastern Anatolia.

Şengör (2006) supports this interpretation and further argues that the increasing alkalinity in volcanism can be explained by thickening of the lithosphere beneath the region. He points out that thickening of lithosphere with the cooling of mantle resulted in deepening of the foci of melting and this increased the alkalinity of the volcanic rocks with time. Although deepening of the foci of melting, in theory, controls the alkalinity of melts in the nature, the magma composition depends more on the composition of the source material. Provided that the source is enriched, deepening of the foci of melting may increase the alkalinity. However, if the source was previously depleted or modified by subducted material, the composition of lavas generated would be dramatically different from those derived from an enriched source. For example, magmas coming from the deep Hawaiian source are mostly tholeiitic. Similarly,

magma generation occurs deep in the mantle wedge beneath island arcs, deeper than most rift settings, but produces calc alkaline lavas reflecting the source chemistry. In the case of the Eastern Anatolian mantle, the source is fairly depleted and appears to have been strongly modified by a subduction component. Therefore, I argue that the increasing alkalinity of lavas in time can be more simply explained by lateral flow of enriched asthenospheric mantle beneath the region. It seems likely that the asthenospheric flow was from the north to the south during the early stages of volcanism in response to the suction effect created by slab-steepening (i.e. an asthenospheric flow from north to south; Figs. 10b,c). This might have carried the subduction-modified and partly-depleted mantle from the north, producing magmas with a subduction signature (Keskin, 2003).

After a certain degree of steepening, the slab appears to have broken off, creating a ‘slab-window’ (Fig. 10c). Hotter asthenosphere once located beneath the slab might have filled this window, generating extensive melting beneath the collision zone along a linear belt. In response to this radical change beneath Eastern Anatolia, asthenospheric mantle flow possibly changed its direction from south to north, bringing hot, enriched and fertile asthenospheric material once located beneath the slab (i.e. underneath the Arabian continent) to shallow depths (Fig. 10d). Shear wave splitting fast polarisation directions (Sandvol et al., 2003b), which display quite a uniform distribution with NE-SW orientations (Fig. 3a) are consistent with the inferred mantle flow direction. This process might have contributed to magma generation and the resultant volcanism in the south around the Muş-Nemrut-Tendürek volcanoes, aligning as a SW-NE trending belt, which is probably sub-parallel to the aforementioned slab-window (Figs. 1 and 2). This may also explain why these volcanoes produced lavas with variable degrees of within-plate signature. Mixing between these two distinct sources (i.e. the partly depleted one containing a subduction component in the north and the enriched one in the south) combined with crustal assimilation and crystallisation (AFC) in crustal chambers may be responsible for generating the great variety of the volcanic material across the region (Fig. 10d).

Recently, in their experimental study Kincaid and Griffiths (2004) showed that steepening of a slab in a subduction system can promote melting both in the mantle wedge and in the slab itself. The results of Kincaid and Griffiths (2004) indicate that a slab-steepening mode of rollback favours steeper flow trajectories into the wedge apex, enhancing decompression melting within the wedge. Flow velocities toward the slab centreline immediately increase by a factor of 3–5 and slab surface temperatures rapidly increase by 100–200°C in this part of the slab. Therefore, slab steepening not only results in melting in the overlying mantle wedge, but also promotes melting in the slab itself. This process might have been important for magma generation beneath the Eastern Anatolian collision zone, possibly during the early stages of the collision-related magmatism.

Another interesting feature of the collision-related units in Eastern Anatolia is that the primitive lavas across the region have trace element and isotopic signatures reflective of a mantle origin, not a crustal origin. Since the accretionary prism had directly overlain hot asthenospheric mantle, one would expect widespread crustal anatexis beneath the region and eruption of lavas with crustal signatures, which does not seem to have been the case for Eastern Anatolian lavas. The numerical modelling studies by Bodorkos et al. (2002) and Gerbi et al. (2006) can provide an answer to this dilemma. Bodorkos et al. (2002) and Gerbi et al. (2006) argue that when the asthenosphere rises to the base of crust in response to the delamination, it significantly heats the crust but cannot cause anatexis. According to Gerbi et al. (2006) the thermal anomaly propagates upward to the middle and upper crust, generating low-pressure metamorphism (550-600 °C at 17 km) within 35 km of the crust, but “not anatexis conditions” in it. If erosion accompanies the lithospheric delamination, the warming effect of the shallow asthenosphere remains limited to the base of the crust. Because the

asthenosphere loses heat, it changes into lithospheric mantle (i.e. a process called the reformation of lithospheric mantle), isolating the crust from the hot asthenosphere (Figs. 10b,c). These findings provide an answer to why collision-related basaltic lavas of Eastern Anatolia have mantle signatures.

The inferred slab-breakoff event might also have been responsible for the regional metamorphism of the Bitlis-Pötürge massif located in the south. The slab-pull effect of the Arabian oceanic lithosphere might have pulled and buried the massif beneath the EAAC, resulting in metamorphism (personal communication with Roland Oberhänsli). Then the massif might have been exhumed right after the slab-breakoff event in response to the loss of a huge lithospheric mass. However, further research is needed to understand the age of metamorphism and its possible link with the slab-breakoff model.

It should be noted that the slab-steepening & breakoff model is viable only if the basement of a greater part of Eastern Anatolia is represented by an accretionary complex (i.e. the EAAC) as proposed by Şengör et al. (2003), and if there was only one north-dipping subducting slab forming this accretionary prism. As the collision-related volcanic sequence masks the basement units over great distances, it is difficult to find evidence that sheds light on whether a great portion of the basement of Eastern Anatolia is represented by the EAAC or not. Interpretation of current surface motion vectors by Şengör (2006) seems to provide an answer to this question. He showed that the deformation style of the area which is presumably covered by the EAAC (he names this area “the squashy zone”) is unique for melange material as it accommodates most of the deformation in the form of thrusts and strike-slip faults, transmitting a relatively smaller fraction of surface movement to rigid continental units in the north (i.e. Pontides and North-west Iranian Fragment). This finding supports the idea that the area masked by volcanic successions is indeed underlain by accretionary prism material.

The slab-steepening and breakoff model proposed for the genesis of the collision-related volcanism in Eastern Anatolia differs from the original model of Davies & von Blanckenburg (1995) since it involves a large accretionary complex and the steepening of the slab beneath it. A number of recent studies address the importance of the slab breakoff process for collision zones (e.g., Nemcok et al., 1998; Chemenda et al., 2000; Maury et al., 2000; Coulon et al., 2002; Haschke et al., 2002; Maheo et al., 2002; Ferrari, 2004; Williams et al., 2004; Molinaro et al., 2005; Knapp et al., 2005; Koulakov, and Sobolev, 2006). The slab-steepening and breakoff process beneath large subduction-accretion complexes, accompanied by magma generation and the emplacement of magmas, may be a very important process in the making of continental crust in ‘Turkic-type’ (Şengör & Natal’in, 1996a) orogenic belts that comprise a large part of the Asian continent (Şengör et al., 2003).

In addition to various processes discussed so far, strike-slip faulting might have played an important role in focusing magmas by generating localized extension and volcanism in associated pull-apart basins (Dewey et al., 1986; Pearce et al., 1990; Keskin et al., 1998). In a recent study, Cooper et al. (2002) support this view and suggest that the mafic magmas beneath NW Tibet might have been created by a mantle upwelling beneath the releasing bends of the strike-slip fault systems. They also present a model for magma generation in such systems. Therefore, like the Tibetan Plateau (e.g., Williams et al., 2004), the uplift and magmatism history of Eastern Anatolia may be related to more than one geodynamic process.

## **6. Conclusion**

The Eastern Anatolian-Iranian high plateau can be regarded as a hot spot or "melting anomaly" coinciding with a regional domal structure which is squeezed in a collision zone in the N-S direction. By virtue of these features, the region closely resembles a mantle plume

setting. However, the Eastern Anatolian domal uplift lies in a collision zone, in contrast to plume-related hot spots located in intraplate settings (e.g., the Ethiopian high plateau).

The Eastern Anatolian lithosphere is, at present, bereft of its mantle component (Şengör et al., 2003). This indicates that a huge piece (perhaps almost the whole thickness) of the mantle lithosphere was detached from the overlying crust in the past. If this removal of the denser mantle material is responsible for both the regional uplift and coeval volcanism, then the detachment must have occurred at about 11-13 Ma, at the same time as onset of those events. The volume opened up by the removal of the mantle lithosphere would have been filled by hot, fertile (i.e. containing a subduction component) asthenospheric upwelling, which would result in both the formation of the regional domal structure (Şengör et al., 2003) and extensive magma generation and volcanism due to adiabatic decompression melting (Keskin, 2003).

On the basis of combined geologic, geophysical and geochemical data, it can thus be argued that the Eastern Anatolian domal uplift (Şengör et al., 2003) is not related to a mantle plume; instead its formation is linked to shallow plate tectonic processes. Temporal and spatial variations in lava chemistry coupled with the uplift history and age relationships of the volcanic products in the Eastern Anatolian Collision Zone may be linked to slab steepening and breakoff beneath a subduction-accretion complex (Şengör et al., 2003; Keskin, 2003) in the south, where the mantle lid is absent (Fig. 9b). Slab steepening was possibly associated with asthenospheric flow that resulted in gradual change in the geochemical character of the volcanics erupted. I argue that lithospheric delamination might still be a more viable model for the northern areas where a lithospheric mantle root, although thinned, still exists (e.g. the Erzurum-Kars Plateau; Fig. 9b). Tomographic sections of Piromallo and Morelli (2003) support this view (Fig. 4d). These two processes can explain the voluminous magma generation and resultant volcanism in addition to formation of the domal uplift across the region better than other competing geodynamic models.

The Eastern Anatolian example is particularly important as it shows that shallow plate tectonic processes can generate both regional lithospheric domal structures and great volumes of magma in the absence of a mantle plume (see also Keskin, 2005). This observation contradicts the proposal of Şengör (2001) who argues that all hotspots and long-wavelength domes on the Earth's surface are related to mantle plumes.

Further research is needed for a better understanding of collision-related magma genesis in Eastern Anatolia and its connection with slab breakoff and other alternative processes. Issues regarding source characteristics, melting mechanisms, the mode and extent of magma-crust interaction and crustal melting also need further investigation.

## **Acknowledgements**

I thank Prof. Gillian R. Foulger for inviting me to contribute to this volume. An earlier version of this paper was presented as a keynote talk at the Chapman Conference: The Great Plume Debate, The Origin of LIPs and Hotspots in Fort William, Scotland in 2005. I am grateful to the Research Fund of Istanbul University for their support (Project No. UDP-589/12072005). I particularly thank Angelo Peccerillo and Ercan Aldanmaz for their helpful comments on an earlier version of this paper. My thanks also go to staff members of the Department of Earth Sciences, Durham University, U.K. for kindly making their research facilities available for me during my sabbatical leave and providing me with a stimulating research environment. Special thanks must also go to the people at St. Chad's College (Durham University) especially to Principal Joseph P. Cassidy and Senior Tutor Margaret Masson for their kindness and generosity during my sabbatical studies. I also thank the people at Ustinov College for their valuable help.

## References

- Al-Damegh, K., Sandvol, E., Al-Lazki, A. and Barazangi, M. (2005). Regional seismic wave propagation (Lg and Sn) and Pn attenuations in the Arabian Plate and surrounding regions, *Geophys. J. Int.*, 157, 775-795.
- Al-Lazki, A., Sandvol, E., Seber, D., Barazangi, M., Türkelli, N. and Mohamad R. (2004). Pn tomographic imaging of mantle lid velocity and anisotropy at the junction of the Arabian, Eurasian and African plates, *Geophys. J. Int.*, 158, 1024-1040.
- Al-Lazki, A., Seber, D., Sandvol, E., Türkelli, N., Mohamad, R. and Barazangi, M. (2003). Tomographic Pn velocity and anisotropy structure beneath the Anatolian plateau (eastern Turkey) and the surrounding regions, *Geophys. Res. Lett.*, 30(24), 8043, doi:10.1029/2003GL017391.
- Allen, M., Jackson, J. and Walker, R. (2004). Late Cenozoic reorganization of the Arabia-Eurasia collision and the comparison of short-term and long-term deformation rates, *Tectonics*, 23, TC2008, doi:10.1029/2003TC001530.
- Anderson, D.L. (2000). The thermal state of the upper mantle: no role for mantle plumes, *Geophys. Res. Lett.*, 27, 3623-3626.
- Anderson, D.L. (2004a). Reheating slabs by thermal conduction in the upper mantle, <http://www.mantleplumes.org/HotSlabs2.html>.
- Anderson, D.L. (2004b). What is a plume?, <http://www.mantleplumes.org/PlumeDLA.html>.
- Angus, D.A., Wilson, D.C., Sandvol, E. and Ni, J.F. (2006). Lithospheric structure of the Arabian and Eurasian collision zone in Eastern Turkey from S-wave receiver functions, *Geophys. J. Int.*, 166 (3): 1335-1346.
- Ateş, A., Kearey, P. and Tufan, S. (1999). New gravity and magnetic anomaly maps of Turkey, *Geophys. J. Int.*, 136, 499–502.
- Balyshv S.O. and Ivanov, A.V. (2001). Low-density anomalies in the mantle: ascending plumes and/or heated fossil lithospheric plates? *Doklady Earth Sciences*, 380, no: 7, 858-862.
- Barazangi, M. (1989). Continental collision zones: Seismotectonics and crustal structure, in *Encyclopedia of Solid Earth Geophysics*, edited by D. James, 58-75, Van Nostrand Reinhold Company, New York.
- Barazangi, M., Sandvol, E., and Seber, D. (2006). Structure and tectonic evolution of the Anatolian plateau in eastern Turkey, in Dilek, Y., and Pavlides, S., eds., *Postcollisional tectonics and magmatism in the Mediterranean region and Asia: GSA Special Paper 409*, p. 463–474, doi: 10.1130/2006.2409(22).
- Becker, T.W., Faccenna, C., O'Connell, R.J. and Giardini, D. (1999). The development of slabs in the upper mantle: insights from numerical and laboratory experiments, *J. Geophys. Res.*, 104, 15,207–15,226.
- Bijwaard, H., Spakman, W. and Engdahl, E.R. (1998). Closing the gap between regional and global travel time tomography, *J. Geophys. Res.*, 103, 30,055– 30,078.
- Bodorkos, S., Sandiford, M., Oliver, N.H.S. and Cawood, P.A. (2002). High-T, low-P metamorphism in the Palaeoproterozoic Hall's Creek Orogen, northern Australia: the middle crustal response to a mantle-related thermal pulse. *J. Metamorphic Geol.*, 20, 217–237.
- Buket, E. and Temel, A. (1998). Major-element, trace-element, and Sr–Nd isotopic geochemistry / and genesis of Varto Muş volcanic rocks, Eastern Turkey, *J. Volc. Geotherm. Res.*, 85, 405–422.
- Chemenda, A.I., Burg, J.P. and Mattauer, M. (2000). Evolutionary model of the Himalaya-Tibet system: geopoem based on new modelling, geological and geophysical data, *Earth Planet. Sci. Lett.*, 174, 397-409.
- Christensen, U.R. (1996). The influence of trench migration on slab penetration into the lower mantle, *Earth Planet. Sci. Lett.*, 140, 27– 39.
- Cooper, K.M., Reid, M.R., Dunbar, N.W. and McIntosh, W.C. (2002). Origin of mafic magmas beneath northwestern Tibet: Constraints from <sup>230</sup>Th–<sup>238</sup>U Disequilibria, *Geochem. Geophys. Geosys.*, 3/1, art. no. 1065.
- Coulon C., Megartsi M., Fourcade, S., Maury, R.C., Bellon, H., Louni-Hacini, A., Cotten, J. Coutelle, A. and Hermitte, D. (2002). Post-collisional transition from calc-alkaline to alkaline

- volcanism during the Neogene in Oranie (Algeria): magmatic expression of a slab breakoff, *Lithos*, 62, 87–110.
- Cruden, A.R., Nasser, M.H.B. and Pysklywec, R. (2006). Surface topography and internal strain variation in wide hot orogens from three-dimensional analogue and two-dimensional numerical vice models, Buitter, S.J.H. & Schreurs, G. (eds), *Analogue and Numerical Modelling of Crustal-Scale Processes*, Geological Society, London, *Special Publications*, 253, 79–104.
- Çakır, Ö. and Erduran, M. (2004). Constraining crustal and uppermost mantle structure beneath station TBZ (Trabzon, Turkey) by receiver function and dispersion analyses, *Geophys. J. Int.*, 158, 955–971.
- Çakır, Ö., Erduran, M., Çınar, H. and Yılmaztürk, A. (2000). Forward modelling receiver functions for crustal structure beneath station TBZ (Trabzon, Turkey), *Geophys. J. Int.*, 140, 341–356.
- Davies, J.H., and von Blanckenburg, F. (1995). Slab breakoff: a model of lithosphere detachment and its test in the magmatism and deformation of collisional orogens, *Earth Planet. Sci. Lett.*, 129, 85–102.
- Dercourt, J., Ricou, L.E. and Vrielynck, B. (Eds.) (1993). *Atlas Tethys, Palaeoenvironmental Maps*, Elsevier, New York.
- Dewey, J.F., Hempton, M.R., Kidd, W.S.F., Şaroğlu, F. and Şengör, A.M.C. (1986). Shortening of continental lithosphere: the neotectonics of Eastern Anatolia – a young collision zone, in *Collision Tectonics*, Geological Society special publications no: 19, edited by M.P. Coward and A.C. Ries, 3–36.
- Elkins-Tanton, L.T. (2004). Continental magmatism caused by lithospheric delamination, <http://www.mantleplumes.org/LithDelam.html>
- England, P.C. and Houseman, G.A. (1988). The mechanics of the Tibetan Plateau, *Philos. Trans. Royal. Soc. London*, A326, 301–320.
- Ercan, T., Fujitani, T., Madsuda, J-I., Notsu, K., Tokel, S. and Tadahide, U.I. (1990). Dogu ve guneydogu Anadolu Neojen-Kuvaterner volkanitlerine iliskin yeni jeokimyasal, radyometrik ve izotopik verilerin yorumu, *M.T.A. Dergisi*, 110, 143–164.
- Ershov, A.V. and Nikishin, A.M. (2004). Recent Geodynamics of the Caucasus–Arabia–East Africa Region, *Geotectonics*, Vol. 38, No. 2, 2004, pp. 123–136.
- Faccenna, C., Bellier, O., Martinod, J., Piromallo, C. and Regard, V. (2006). Slab detachment beneath eastern Anatolia: A possible cause for the formation of the North Anatolian fault, *Earth Planet. Sci. Lett.*, 242, 85–97.
- Ferrari, L. (2004). Slab detachment control on mafic volcanic pulse and mantle heterogeneity in central Mexico, *Geology*, 32; no. 1, 77–80, DOI 10.1130/G19887.1.
- Foulger, G.R. and Natland, J.H. (2003). Is 'hotspot' volcanism a consequence of plate tectonics? *Science*, 300: 921.
- Foulger, G.R. (2002). Plumes or plate tectonic processes? *Astron. Geophys.*, 43, 6.19–6.23.
- Foulger, G.R., Natland, J.H. and Anderson, D.L. (2005). A source for Icelandic magmas in remelted Iapetus crust, *J. Volc. Geotherm. Res.*, 141, 23–44.
- Gaherty, J.B. and Hager, B.H. (1994). Compositional vs. thermal buoyancy and the evolution of subducted lithosphere, *Geophys. Res. Lett.*, 21, 141–144.
- Gasparik, T. (1997). A model for the layered upper mantle, *Phys. Earth Planet. Int.*, 100, 197–212.
- Gelati, R. (1975). Miocene marine sequence from Lake Van, Eastern Turkey, *Riv. Ital. Paleont. Stratigr.*, 81, 477–490.
- Gerbi, C.C., Johnson, S.E. and Koons, P.O. (2006). Controls on low-pressure anatexis, *J. Metamorphic Geol.*, 2006, 24, 107–118, doi:10.1111/j.1525-1314.2005.00628.x
- Gök, R., Sandvol, E., Türkelli, N., Seber, D. and Barazangi, M. (2003). Sn attenuation in the Anatolian and Iranian plateau and surrounding regions, *Geophys. Res. Lett.*, 30(24), 8042, doi:10.1029/2003GL018020.
- Gök, R., Türkelli, N., Sandvol, E., Seber, D. and Barazangi, M. (2000). Regional wave propagation in Turkey and surrounding regions, *Geophys. Res. Lett.*, 27(3), 429–432.
- Hafkenscheid, E., Wortel, M.J.R. and Spakman, W. (2006). Subduction history of the Tethyan region derived from seismic tomography and tectonic reconstructions, *J. Geophys. Res.*, -*Solid Earth*, 111 (B8): Art. No. B08401.

- Haschke, M.R., Scheuber, E., Gunther, A. and Reutter, K.-J. (2002). Evolutionary cycles during the Andean orogeny: repeated slab breakoff and flat subduction?, *Terra Nova*, 14, 49-55.
- Hearn, T.N., and Ni, J.F. (1994). Pn velocities beneath continental collision zones: The Turkish-Iranian Plateau, *Geophys. J. Int.*, 117, 273-283.
- Housman, G.A., McKenzie, D.P. and Molnar, P. (1981). Convective instability of a thickened boundary layer and its relevance for the thermal evolution of continental collision belts, *J. Geophys. Res.*, 86, 6115-6132.
- Innocenti, F., Manetti, P., Mazzuoli, R., Pasquaré, G. and Villari, L. (1982a). Anatolia and north-western Iran, in *Andesites*, Ed. R.S. Thorpe, John Wiley & Sons.
- Innocenti, F., Mazzuoli, R., Pasquaré, G., Radicati di Brozolo, F. and Villari, L. (1982b). Tertiary and Quaternary volcanism of the Erzurum-Kars area (Eastern Turkey): Geochronological data and geodynamic evolution, *J. Volc. Geotherm. Res.*, 13, 223-240.
- Irvine, T.N. and Baragar, W.R.A. (1971). A guide to the chemical classification of the common volcanic rocks, *Canadian J. Earth Sci.*, 8, 523-548.
- Ivanov, A.V. (2003). Plumes or reheated slabs?, <http://www.mantleplumes.org/HotSlabs1.html>.
- Karapetian, S.G., Jrbashian, R.T. and Mnatsakanian, A.K. (2001). Late collision rhyolitic volcanism in the north-eastern part of the Armenian Highland, *J. Volc. Geotherm. Res.*, 112 (1-4), 189-220.
- Kaufman, P.S. and Royden, L.H. (1994). Lower crustal flow in an extensional setting: Constraints from the Halloran Hills region, eastern Mojave Desert, California. *J. Geophys. Res.*, 99, 15723-15739.
- Keskin, M. (1994). Genesis of collision-related volcanism on the Erzurum-Kars Plateau, Northeastern Turkey, Unpublished PhD thesis, Univ. Durham, U.K.
- Keskin, M. (2002). FC-Modeler: a Microsoft® Excel® spreadsheet program for modeling Rayleigh fractionation vectors in closed magmatic systems, *Computers & Geosciences*, 28/8, 919-928.
- Keskin, M. (2003). Magma generation by slab steepening and breakoff beneath a subduction-accretion complex: An alternative model for collision-related volcanism in Eastern Anatolia, Turkey, *Geophys. Res. Lett.*, 30(24), 8046, doi:10.1029/2003GL018019.
- Keskin, M. (2005). Domal uplift and volcanism in a collision zone without a mantle plume: Evidence from Eastern Anatolia, URL: <http://www.mantleplumes.org/Anatolia.html>
- Keskin, M., Pearce, J.A. and Mitchell, J.G. (1998). Volcano-stratigraphy and geochemistry of collision-related volcanism on the Erzurum-Kars Plateau, North Eastern Turkey, *J. Volc. Geotherm. Res.*, 85(1-4), 355-404.
- Keskin, M., Pearce, J.A., Kempton, P.D. and Greenwood, P. (2006). Magma-crust interactions and magma plumbing in a post-collision setting: Geochemical evidence from the Erzurum-Kars Volcanic Plateau, Eastern Turkey, in Dilek, Y., and Pavlides, S., eds., Postcollisional tectonics and magmatism in the Mediterranean region and Asia: *Geol. Soc. Amer. Spec. Paper* 409, 475-505, doi: 10.1130/2006.2409(23).
- Kincaid, C. and Griffiths, R.W. (2004). Variability in flow and temperatures within mantle subduction zones, *Geochemistry Geophysics Geosystems*, 5: Art. No. Q06002.
- Knapp J.H., Knapp, C.C., Raileanu, V., Matenco, L., Mocanu, V. and Dinu, C. (2005). Crustal constraints on the origin of mantle seismicity in the Vrancea Zone, Romania: The case for active continental lithospheric delamination, *Tectonophysics*, 410, 311-323.
- Koronovskiy, N.V. and Demina, L.I. (1996). A model for the collision volcanism of the Caucasian segment of the Alpine Fold Belt, *Dokl. Akad. Nauk Rossi.*, 350, 519-522 (in Russian).
- Koulakov, I. and Sobolev, S.V. (2006). A tomographic image of Indian lithosphere break-off beneath the Pamir-Hindukush region, *Geophys. J. Int.*, 164, 425-440.
- Kuno, H. (1966). Lateral variation of basalt magma types across continental margins and island arcs, *Bull. Volcanol.*, 29, 195-222.
- Lay, T. (1994). The fate of descending slabs, *Annu. Rev. Earth Planet. Sci.*, 22, 33-61.
- Lustrino, M. (2005). How the delamination and detachment of lower crust can influence basaltic magmatism, *Earth Sci. Reviews*, 72 (1-2), 21-38.
- Maggi A. and Priestley, K. (2005). Surface waveform tomography of the Turkish-Iranian plateau, *Geophys. J. Int.*, 160 (3): 1068-1080.

- Maggi, A., Priestley, K. and McKenzie, D. (2002). Seismic structure of the Middle East, *Eos Trans. AGU*, 83(47), *Fall Meet. Suppl.*, Abstract S51B-1041.
- Maheo, G., Guillot, S., Blichert-Toft, J., Rolland, Y. and Pecher, A. (2002). A slab breakoff model for the Neogene thermal evolution of South Karakorum and South Tibet, *Earth Planet. Sci. Lett.*, 195(1-2), 45-58.
- Maury, R.C., Fourcade, S., Coulon, C., El Azzouzi, M., Bellon, H., Coutelle, A., Oubadi, A., Semroud, B., Megartsi, M., Cotton, J., Belanteur, Q., Louni-Hacini, A., Pique, A., Capdevila, R., Hernandez, J. and Rehaulp, J.P. (2000). Post-collisional Neogene magmatism of the Mediterranean Maghreb margin: a consequence of slab breakoff, *Comptes Rendus de la Academie Des Sciences Serie II Fascicule A Sciences de la Terre et des Planets*, 331(3), 159-173.
- McKenzie, D.P. (1972). Active tectonics of the Mediterranean, *Geophys. J. R. Astr. Soc.*, 30(2), 109-185.
- McKenzie, D.P., and Bickle, M.J. (1988). The volume and composition of melt generated by extension of the lithosphere, *J. Pet.*, 29, 625-679.
- Mitchell, J. and Westaway, R. (1999). Chronology of Neogene and Quaternary uplift and magmatism in the Caucasus: constraints from K - Ar dating of volcanism in Armenia, *Tectonophysics*, 304, 157-186.
- Molinaro, M., Zeyen, H. and Laurencin, X. (2005). Lithospheric structure beneath the south-eastern Zagros Mountains, Iran: recent slab break-off?, *Terra Nova*, 17, 1-6, doi: 10.1111/j.1365-3121.2004.00575.x.
- National Iranian Oil Company (1977). Geological cross-sections north-west Iran, Natl. Iranian Oil Co., Tehran.
- Nemcok, M., Pospisil, L., Lexa, J. and Donelick, R.A. (1998). Tertiary subduction and slab break-off model of the Carpathian-Pannonian region, *Tectonophysics*, 295, 307-340.
- Notsu, K., Fujitani, T., Ui, T., Matsuda, J. and Ercan, T. (1995). Geochemical features of collision-related volcanic rocks in central and eastern Anatolia, Turkey, *J. Volcanol. Geotherm. Res.*, 64, 171-192.
- Özdemir, Y., Karaoğlu, O., Tolluoğlu, A.U. and Güleç, N. (2006). Volcanostratigraphy and petrogenesis of the Nemrut stratovolcano (East Anatolian High Plateau): the most recent post collisional volcanism in Turkey, *Chem. Geol.*, in press.
- Pearce, J.A. (1983). Role of the sub-continental lithosphere in magma genesis at active continental margins, *In Continental Basalts and Mantle Xenolites* (C.J. Hawkesworth and M.J. Norry, eds), Shiva, Nantwich, 230-249.
- Pearce, J.A., Bender, J.F., De Long, S.E., Kidd, W.S.F., Low, P.J., Güner, Y., Şaroğlu, F., Yılmaz, Y., Moorbath, S. and Mitchell, J.G. (1990). Genesis of collision volcanism in Eastern Anatolia, Turkey, *J. Volcanol. Geotherm. Res.*, 44, 189-229.
- Peccerillo, A. and Taylor, S.R. (1976). Geochemistry of Eocene calc-alkaline volcanic rocks from the Kastamonu area, northern Turkey, *Contrib. Mineral. Petrol.*, V. 58, pp. 63-81.
- Peccerillo, A., Barberio, M.R., Yirgu, G., Ayalew, D., Barbieri, M. and Wu, T.W. (2003). Relationship between mafic and peralkaline silicic magmatism in continental rift settings: a petrological, geochemical and isotopic study of the Gedemsa volcano, Central Ethiopian Rift, *J. Petrol.*, 44, no: 11, 2003-2032, DOI: 10.1093/petrology/egg068.
- Piromallo, A. and Morelli, P. (2003). P wave tomography of the mantle under the Alpine-Mediterranean area, *J. Geophys. Res.*, 108, doi: 10.1029/2002JB001757.
- Platt, J.P. and England, P.C. (1993). Convective removal of lithosphere beneath mountain belts: Thermal and mechanical consequences. *Am. J. Sci.*, 293, 307-336.
- Regard, V., Faccenna, C., Martinod, J. and Bellier, O. (2005). Slab pull and indentation tectonics: insights from 3D laboratory experiments, *Physics of the Earth and Planetary Interiors*, 149, 99-113.
- Regard, V., Bellier, O., Martinod, J. and Faccenna, C. (2006). Analogue experiments of subduction vs. collision processes: insight for the Iranian tectonics, *JSEE: Fall 2005*, Vol. 7, No. 3 / 1-9.
- Reilinger, R., McClusky, S., Oral, B., King, R., Toksoz, N., Barka, A., Kınık, I., Lenk, O. and Şanlı, I. (1997). Global positioning system measurements of present-day crustal movements in the Arabia-Africa-Eurasia plate collision zone, *J. Geophys. Res.*, 102 (B5), 9983-9999.

- Reilinger, R., McClusky, S., Vernant, P., Lawrence, S., Ergintav, S., Çakmak, R., Özener, H., Kadirov, F., Guliev, I., Stepanyan, R., Nadariya, M., Hahubia, G., Mahmoud, S., Sakr, K., ArRajehi, A., Paradissis, D., Al-Aydrus, A., Prilepin, M., Guseva, T., Evren, E., Dmitrotsa, A., Filikov, S.V., Gomez, F., Al-Ghazzi, R. and Karam, G. (2006). GPS constraints on continental deformation in the Africa-Arabia-Eurasia continental collision zone and implications for the dynamics of plate interactions, *J. Geophys. Res.*, 111, B05411, doi:10.1029/2005JB004051.
- Rotstein, Y., and Kafka, A.L. (1982). Seismotectonics of the southern boundary of Anatolia, eastern Mediterranean region, subduction, collision and arc jumping, *J. Geophys. Res.*, 87, 7694-7706.
- Sandvol, E., Seber, D., Barazangi, M., Türkelli, N., Gürbüz, C., Kuleli, S., Karabulut, H., Zor, E., Gök, R., Bekler, T., Arpat, E. and Bayraktutan, S. (2000). Eastern Turkey Seismic Experiment, *IRIS Newsletter*, 2000(1).
- Sandvol, E., Türkelli, N. and Barazangi, M. (2003a). The Eastern Turkey Seismic Experiment: The study of a young continent-continent collision, *Geophys. Res. Lett.*, 30(24), 8038, doi:10.1029/2003GL018912.
- Sandvol, E., Türkelli, N., Zor, E., Gök, R., Bekler, T., Gürbüz, C., Seber, D. and Barazangi, M. (2003b). Shear wave splitting in a young continent-continent collision: An example from Eastern Turkey, *Geophys. Res. Lett.*, 30(24), 8041, doi:10.1029/2003GL017390.
- Sandvol, E. and Zor, E. (2004). Upper mantle P and S-wave velocity structure beneath eastern Anatolian plateau, EOS, *Trans. Am. geophys. Un.*, AGU Fall Meeting 2004, S13B-1056.
- Stampfli, G.M. and Borel, G.D. (2002). A plate tectonic model for the Paleozoic and Mesozoic constrained by dynamic plate boundaries and restored synthetic oceanic isochrons, *Earth Planet. Sci. Lett.*, 196, 17-33.
- Stampfli, G.M. and Borel, G.D. (2004). The TRANSMED transects in space and time: Constraints on the paleotectonic evolution of the Mediterranean domain, in *The TRANSMED Atlas: The Mediterranean Region from Crust to Mantle*, (W. Cavazza et al. eds.), 53- 80, Springer, New York.
- Sun, S.S. and McDonough, W.F. (1989). Chemical and isotopic systematics of oceanic basalts: implications for mantle composition and processes: In *Magmatism in Ocean Basins* (A.D. Saunders & M.J. Norry eds.), *Geol. Soc. Lond. Spec. Pub.*, 42, 313-345.
- Şen, P.A., Temel, A. and Gourgaud, A. (2004). Petrogenetic modelling of Quaternary post-collisional volcanism: a case study of central and eastern Anatolia, *Geol. Mag.*, 141(1), 81-98, DOI: 10.1017/S0016756803008550.
- Şengör, A.M.C. (1990). A new model for the late Palaeozoic-Mesozoic tectonic evolution of Iran and implications for Oman, in *The Geology and Tectonics of the Oman Region*, (A.H.F. Robertson, M.P. Searle and A.C. Ries eds.), *Geol. Soc. Spec. Publ.*, 49, 797 - 831.
- Şengör, A.M.C. (2001). Elevation as indicator of mantle-plume activity, *Geol. Soc. Am., Sp. Pap.*, 352, 183-225.
- Şengör, A.M.C. (2002). The Turkish-Iranian High Plateau as a falcogenetic structure, *Workshop on the Tectonics of Eastern Turkey and the Northern Anatolian plate*, Erzurum, Turkey, p. 28.
- Şengör, A.M.C. (2006). Tectonics of the Turkish-Iranian High Plateau, *Lake Van Drilling Project (ICDP), PaleoVan Workshop in Van, Turkey*, June 6 - 9, 2006.
- Şengör, A.M.C. and Kidd, W.S.F. (1979). Post-collisional tectonics of the Turkish-Iranian Plateau and a comparison with Tibet, *Tectonophysics*, 55, 361-376.
- Şengör, A.M.C. and Natal'in, B.A. (1996a). Turkic-type orogeny and its role in the making of the continental crust, *Annu. Rev. Earth Planet. Sci.*, 24, 263-337.
- Şengör, A.M.C. and Natal'in, B.A. (1996b). Paleotectonics of Asia: Fragments of a synthesis, in *The Tectonic Evolution of Asia*, (A. Yin and T. M. Harrison eds.), 486- 640, Cambridge Univ. Press, New York.
- Şengör, A.M.C., and Yılmaz, Y. (1981). Tethyan evolution of Turkey: a plate tectonic approach, *Tectonophysics*, 75, 181-241.

- Şengör, A.M.C., Özeren, S., Zor, E. and Genç, T. (2003). East Anatolian high plateau as a mantle-supported, N-S shortened domal structure, *Geophys. Res. Lett.*, 30(24), 8045, doi:10.1029/2003GL017858.
- Taylor, S.R. and McLennan, S.M. (1985). *The continental crust: its composition and evolution*, Geoscience Texts, Blackwell Scientific Publications, London, 312 pp.
- Tokel, S. (1985). Mechanism of crustal deformation and petrogenesis of the Neogene volcanics in East Anatolia, *Special Publication of Türkiye Jeoloji Kurumu, Ketin Symposium* (Eds. T. Ercan and M.A. Caglayan), 121-130.
- Topuz, G., Altherr, R., Kalt, A., Satır, M., Werner, O. and Schwarz, W.H. (2004). Aluminous granulites from the Pulur complex, NE Turkey: a case of partial melting, efficient melt extraction and crystallization, *Lithos*, 72, 183-207.
- Türkoğlu, E., Unsworth, M., Çağlar, I., Tuncer, V., Avşar, U. and Tank, B., Türkoğlu, E., Demir, T. and Şener, A. (2005). Electrical resistivity structure of the Arabia-Eurasia Collision Zone in Eastern Anatolia, AGU 2005, T51C-1350.
- Türkoğlu, E., Unsworth, M., Çağlar, I., Tuncer, V., Avşar, U. and Tank, B. (2006). Magnetotelluric imaging of the Eurasian-Arabian collision in Eastern Anatolia, *IAGA WG 1.2 on Electromagnetic Induction in the Earth, Extended Abstract 18 Workshop*, El Vendrell, Spain, September, 17-23.
- Turcotte, D.L. (1983). Mechanism of crustal deformation, *J. Geol. Soc. Lond.*, 140, 701-724.
- Türkelli, N., Sandvol, E., Zor, E., Gök, R., Bekler, T., Al-Lazki, A., Karabulut, H., Kuleli, S., Eken, T., Gürbüz, C., Bayraktutan, S., Seber, D. and Barazangi, M. (2003). Seismogenic zones in Eastern Turkey, *Geophys. Res. Lett.*, 30(24), 8039, doi:10.1029/2003GL018023.
- Williams, H.M., Turner, S.P., Pearce, J.A., Kelley, S.P. and Harris, N.B.W. (2004). Nature of the source regions for post-collisional, potassic magmatism in Southern and Northern Tibet from geochemical variations and inverse trace element modeling, *J. Pet.*, 45(3), 555-607.
- Yılmaz Y., Güner Y. and Şaroğlu, F. (1998). Geology of the quaternary volcanic centers of the east Anatolia, *J. Volc. Geotherm. Res.*, 85(1-4), 173-210.
- Yılmaz, Y., Tüysüz, O., Yiğitbaş, E., Genç, S.C. and Şengör, A.M.C. (1997). Geology and tectonic evolution of the Pontides, in *Regional and Petroleum geology of the Black Sea and Surrounding Region*, Ed. A.G. Robinson, *AAPG Memoir*, 68, 183-226.
- Zor, E., Gürbüz, C., Türkelli, N., Sandvol, E., Seber, D. and Barazangi, M. (2003). The crustal structure of the East Anatolian Plateau from receiver functions, *Geophys. Res. Lett.*, 30(24), 8044, doi:10.1029/2003GL018192.

## FIGURE CAPTIONS

**Figure 1.** (a) Simplified geological map of Eastern Anatolia showing tectonic units, collision-related volcanic products and volcanic centres. E-K-P: the Erzurum-Kars Plateau; NATF and EATF: North and East Anatolian Transform Faults. Volcanic centers: Ag: Mt. Ağrı (Ararat), Al<sup>1</sup>: Mt. Aladağ (SE of Ağrı), Al<sup>2</sup>: Mt. Aladağ (NW of Horasan), Bi: Mt. Bingöl, Bl: Mt. Bilicandağı, D: Mt. Dumanlıdağ, E: Mt. Etrüsk, H: Mt. Hamadağ, K: Mt. Karatepe, Ki: Mt. Kısırdağ, M: Mt. Meydandağ, N: Mt. Nemrut, S: Mt. Süphan, T: Mt. Tendürek, Y: Mt. Yağlıcadağ, Z: Mt. Ziyaretdağ.

(b) Major tectonic blocks of Eastern Anatolia. The borders are modified from Şengör et al. (2003). I: Rhodope-Pontide fragment, II: Northwest Iranian fragment, III: Eastern Anatolian Accretionary Complex (EAAC), IV: Bitlis-Pötürge Massif, V: Arabian foreland. Dark green areas: outcrops of ophiolitic melange, Pink and red areas: collision-related volcanic units, white areas: undifferentiated units or young cover formations. EKP: the Erzurum-Kars Plateau in the north.

(c) Distribution of the oldest radiometric ages of the volcanic units. Ages are from Pearce et al. (1990), Ercan et al. (1990) and Keskin et al. (1998). Initiation ages of the volcanism are

contoured in 1-Myr intervals. PS: Pontide suture, BPS: Bitlis-Pötürge suture, CS: inferred cryptic suture between the EAAC and the Bitlis-Pötürge Suture (BPS).

**Figure 2.** MrSID satellite view of major volcanic centers of Eastern Anatolia. (a) Mt. Aladağ volcano on the Erzurum-Kars Plateau, (b) a general view of the Erzurum-Kars Plateau in the northernmost part of Eastern Anatolia, (c) Mt. Ararat: a double-peaked stratovolcano and (d) Tendürek: a shield volcano in the northeast, (e) Mt. Nemrut volcano in the south, (f) Süphan stratovolcano in the north of Lake Van, and (g) Bingöl volcano: a truncated volcano by the North Anatolian Transform Fault (i.e. NATF). Reddish-brownish coloured areas correspond to volcanic units, while purple to pinkish areas are either basement units (e.g., areas in the northwest) or young sedimentary cover formations. Vegetation is in general represented by green areas. For the legend of the inset map, see Fig. 1a.

**Figure 3.** (a) The map showing collision-related volcanic and tectonic units, mantle lid thicknesses and shear wave splitting fast polarisation directions (from Fig. 1 of Sandvol et al., 2003b) in Eastern Anatolia. Contours (red) indicate the mantle lid (i.e. lithospheric mantle) thicknesses in km (contours are from Fig. 2 of Şengör et al., 2003). The light bluish-coloured triangular area surrounded by the cities of Ağrı, Erzurum, Bingöl and Van in the centre of the figure represents the area with no mantle lid. Thick, dotted dark blue lines represent the northern and southern borders of the Eastern Anatolian Accretionary Complex (also see Fig. 1b). Note that areas of inferred complete lithospheric detachment almost exactly coincide with the extent of the Eastern Anatolian Accretionary Complex (i.e. the EAAC).

(b). Cross section summarizing the lithospheric structure across Eastern Anatolia (not to scale). The crustal and lithospheric thicknesses are from Şengör et al. (2003) and Zor et al. (2003). The direction of the cross section (A-A') is shown in (a). Source of geochemical data: Ercan et al. (1990), Pearce et al. (1990), Keskin et al. (1998). SC: subduction component, F: strike-slip faults.

**Figure 4.** Tomographic cross sections showing the lithospheric structure of Eastern Anatolia (b to e) (Maggi and Priestly, 2005; Piromallo and Morelli, 2003). An E-W topographic profile along the 40°N parallel (Şengör et al., 2003) is also presented above the figure (a). The smooth line in 'a' represents least squares simplifications of the topography.

**Figure 5.** Major-oxide and trace-element diagrams for classifying the lavas of Eastern Anatolia. (a to c) Classification of volcanic units of Eastern Anatolia on the total alkali vs. silica diagram of Le Bas et al. (1986). Data for Erzurum-Kars Plateau are from Keskin et al. (1998) and from Pearce et al. (1990). Data for Bingöl-Süphan are from Pearce et al. (1990) and Notsu et al. (1995), while the data for Muş-Nemrut-Tendürek are taken from Pearce et al. (1990), Buket and Temel (1998) (only for Muş), Şen et al. (2004) (only for Tendürek), and Özdemir et al. (2006) (only for Nemrut). Diagrams are arranged from north to south: the Erzurum-Kars plateau in the north, Bingöl-Süphan areas in the central-west, Muş-Nemrut-Tendürek areas in the south. Abbreviations: B: basalt, BA: basaltic andesite, TB: trachybasalt, BTA: basaltic trachyandesite, A: andesite, TA: trachyandesite, D: dacite, TD: trachydacite, T: trachite, R: rhyolite, IB: alkaline/subalkaline divide of Irvine and Baragar (1971), Ku: alkaline/sub-alkaline divide of Kuno (1966). Alkalinity increases from north to the south.

(d to f) Classification of the volcanic units of Eastern Anatolia on the K<sub>2</sub>O vs. silica diagram of Peccerillo & Taylor (1976). Data sources are the same as described above (i.e. a to c).

(g to i) N-type MORB-normalised patterns for volcanic samples from the Eastern Anatolia collision zone. Normalisation values are from Sun and McDonough (1989). Source of the data is presented in the inset of each diagram. Numbers in brackets in the legend of "g" are SiO<sub>2</sub>

wt. % values. The elements are arranged in the order suggested by Pearce (1983). Note that the samples from the Erzurum-Kars Plateau in the north contain a distinct subduction signature, while lavas of the Muş-Nermrut-Tendürek areas display an intraplate signature with or without a slight subduction signature. Samples from the Bingöl-Süphan area display intermediate characteristics between the Erzurum-Kars Plateau and the Muş-Nermrut-Tendürek areas. Data sources are the same as described above (i.e. a to c).

**Figure 6.** Trace-element diagrams used to study spatial variations in the petrogenesis and geochemistry of the lavas of Eastern Anatolia.

(a to c) Th/Yb vs. Ta/Yb diagrams (after Pearce, 1983) for basic and intermediate lavas ( $\text{SiO}_2 < 60\%$ ) from the Eastern Anatolia Collision Zone. Data sources are the same as described in the caption of Fig. 5a to c. MM: mantle metasomatism array; SZE: subduction zone enrichment; WPE: within-plate enrichment; UC: upper crustal composition of Taylor & McLennan (1985); FC: fractional crystallisation vector; AFC: assimilation combined with fractional crystallisation curve. The FC curve has been modelled for 50% crystallisation of an assemblage consisting of 50% plagioclase and 50% amphibole from a basic magma. The AFC vector has been drawn for an "r" value of 0.3. Note that this kind of diagram is not useful for differentiating FC process from AFC. Lavas of the Erzurum-Kars Plateau contain a distinct subduction zone enrichment (SZE) signature.

(d and e). Th/Ta vs. MgO and Ta diagrams, highlighting the spatial variations in the geochemistry of lavas across the region. Data sources are the same as described in the caption of Fig. 5a to c. For an explanation, see the text.

(f to h). Rb vs. Y diagrams displaying theoretical Rayleigh fractionation vectors for 50% crystallisation of the phase combinations (given below) from a common magma composition. Tick marks on each vector correspond to 5% crystallisation intervals. Data sources are the same as described in the caption of Fig. 5a to c. Bulk partition coefficient values used in the modelling are those given in Table 2 of Keskin et al. (1998). The FC vectors have been modelled using the 'FC-Modeler program' of Keskin (2002). Phase combinations for the vectors: 1. plg<sub>5</sub>+cpx<sub>3</sub>+olv<sub>2</sub> (B); 2. plg<sub>5</sub>+cpx<sub>5</sub> (B) or ~plg<sub>5</sub>+cpx<sub>3</sub>+olv<sub>2</sub> (I); 3. plg<sub>5</sub>+amp<sub>5</sub> (B) or plg<sub>5</sub>+cpx<sub>5</sub> (I) 4. plg<sub>2</sub>+opx<sub>1</sub>+cpx<sub>6</sub>+olv<sub>1</sub> (I); 5. plg<sub>5</sub>+cpx<sub>5</sub> (A); 6. plg<sub>5</sub>+amp<sub>5</sub> (I); 7. plg<sub>4</sub>+amp<sub>4</sub>+gt<sub>2</sub> (I); 8. plg<sub>5</sub>+amp<sub>5</sub> (A); 9. plg<sub>4</sub>+amp<sub>4</sub>+gt<sub>2</sub> (A). plg: plagioclase, cpx: clinopyroxene, opx: orthopyroxene, olv: olivine, amp: amphibole, gt: garnet. B: basic, I: intermediate, and A: acid magma compositions.

**Figure 7.** Competing geodynamic models proposed for Eastern Anatolia.

**Figure 8.** Block diagrams illustrating the delamination model for the Eastern Anatolian Collision Zone. Modified from Keskin (1994).

**Figure 9.** Block diagrams illustrating the slab-steepening & breakoff model for the Eastern Anatolian Collision Zone. SC: subduction component. White arrows indicate possible flow direction of the asthenosphere. Modified from Şengör et al. (2003). Also see Fig. 3 of Keskin (2003).

**Figure 10.** Cross sections displaying the evolution of the Eastern Anatolian collision zone in time. EAAC: the Eastern Anatolian Accretionary Complex; ALM: Arabian lithospheric mantle, BPLM: lithospheric mantle of the Bitlis-Pötürge Massif, PLM: lithospheric mantle of the Pontides, SC: asthenospheric mantle containing a subduction component, F: strike-slip faults.

## TABLE CAPTION

**Table 1.** Table of major, trace element and isotopic data on representative rock types across Eastern Anatolia. Data source: Buk-Tem: Buket and Temel (1998); Keskin: Keskin et al. (1998 and 2006); Özdemir: Özdemir et al. (2006); Pearce: Pearce et al. (1990); Sen: Şen et al. (2004).

Abbreviations: Ba: basalt; BaAnd: basaltic-andesite; BaTrAnd: basaltic trachy-andesite; And: andesite; TrAnd: trachy-andesite; Dac: dacite; TrDac: trachy-dacite; and Rhy: rhyolite.

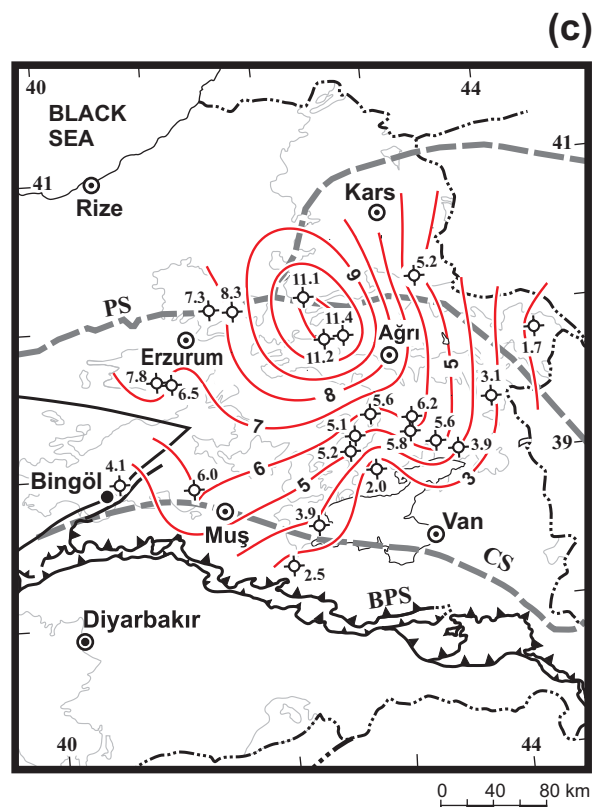
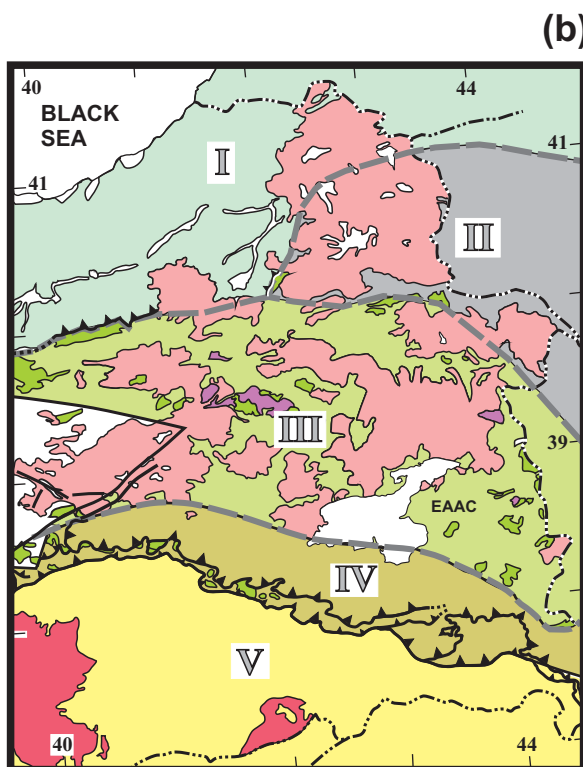
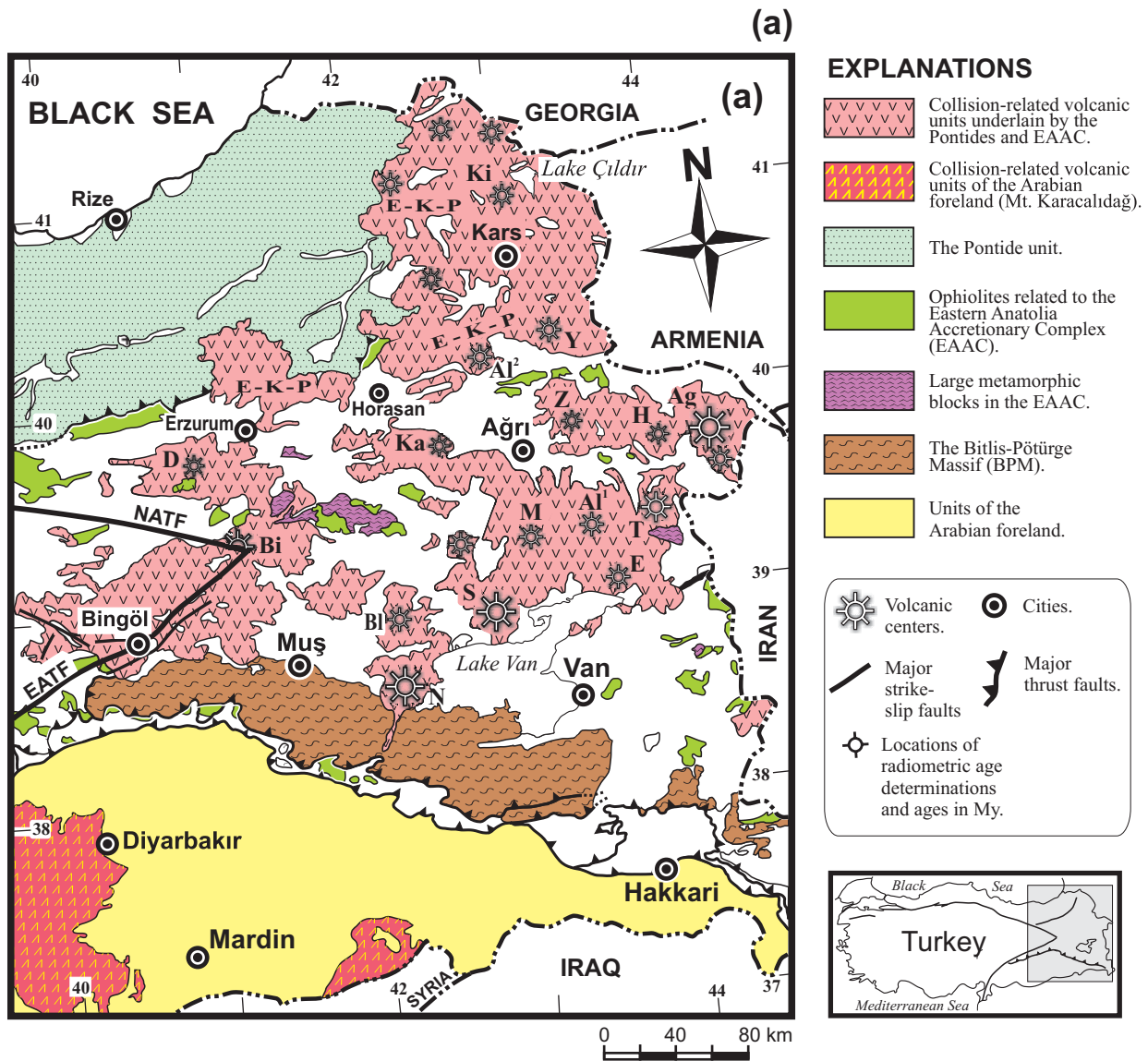
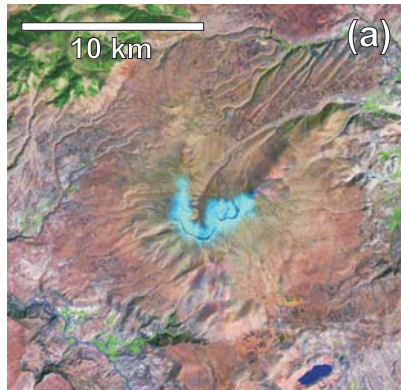
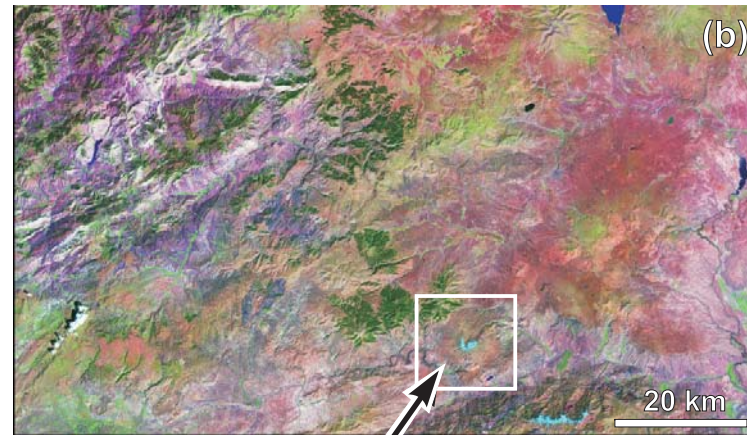


Figure: 1.

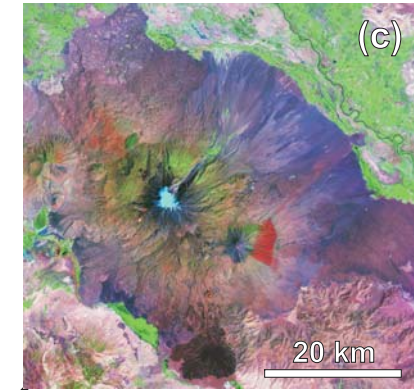
**Aladağ volcano on the EKP**



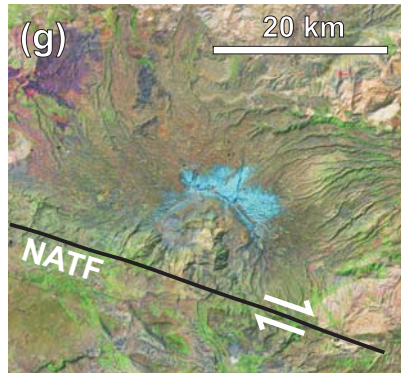
**Erzurum-Kars Plateau (EKP)**



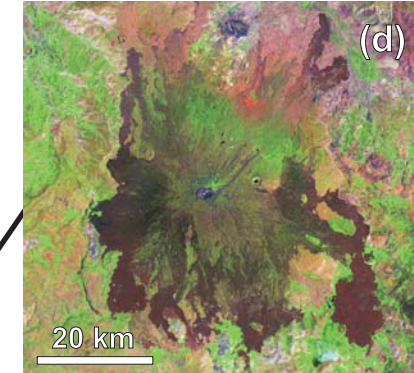
**Mt. Ararat**



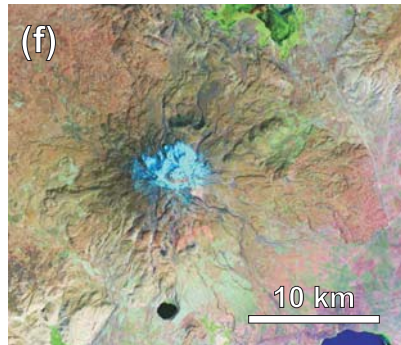
**Bingöl volcano**



**Tendürek volcano**



**Süphan volcano**



**Nemrut volcano**

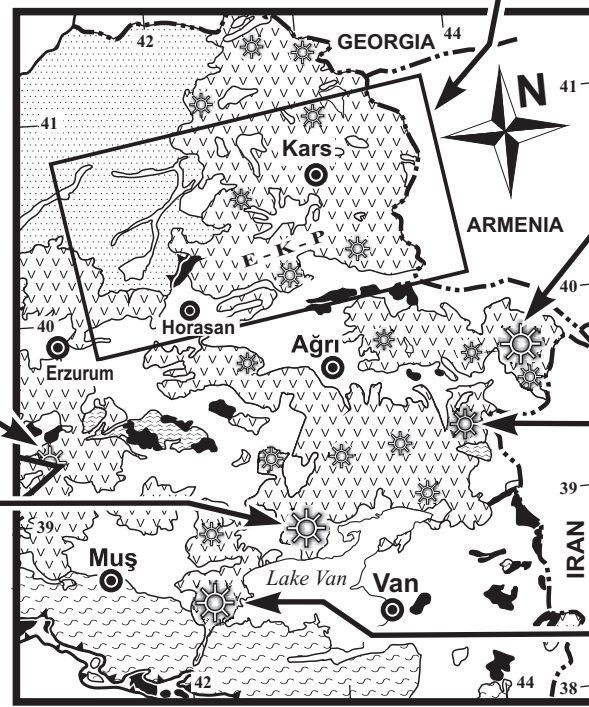


**Figure: 2.**

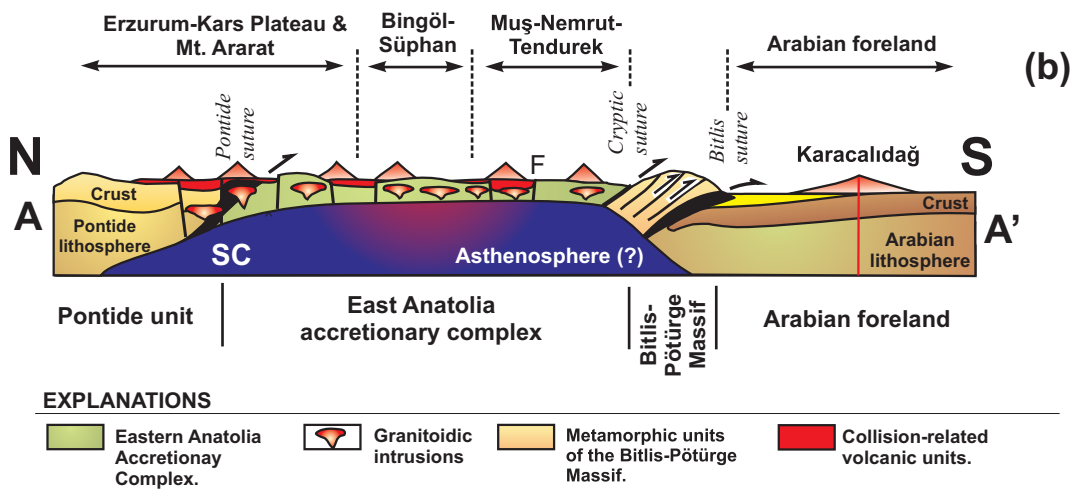
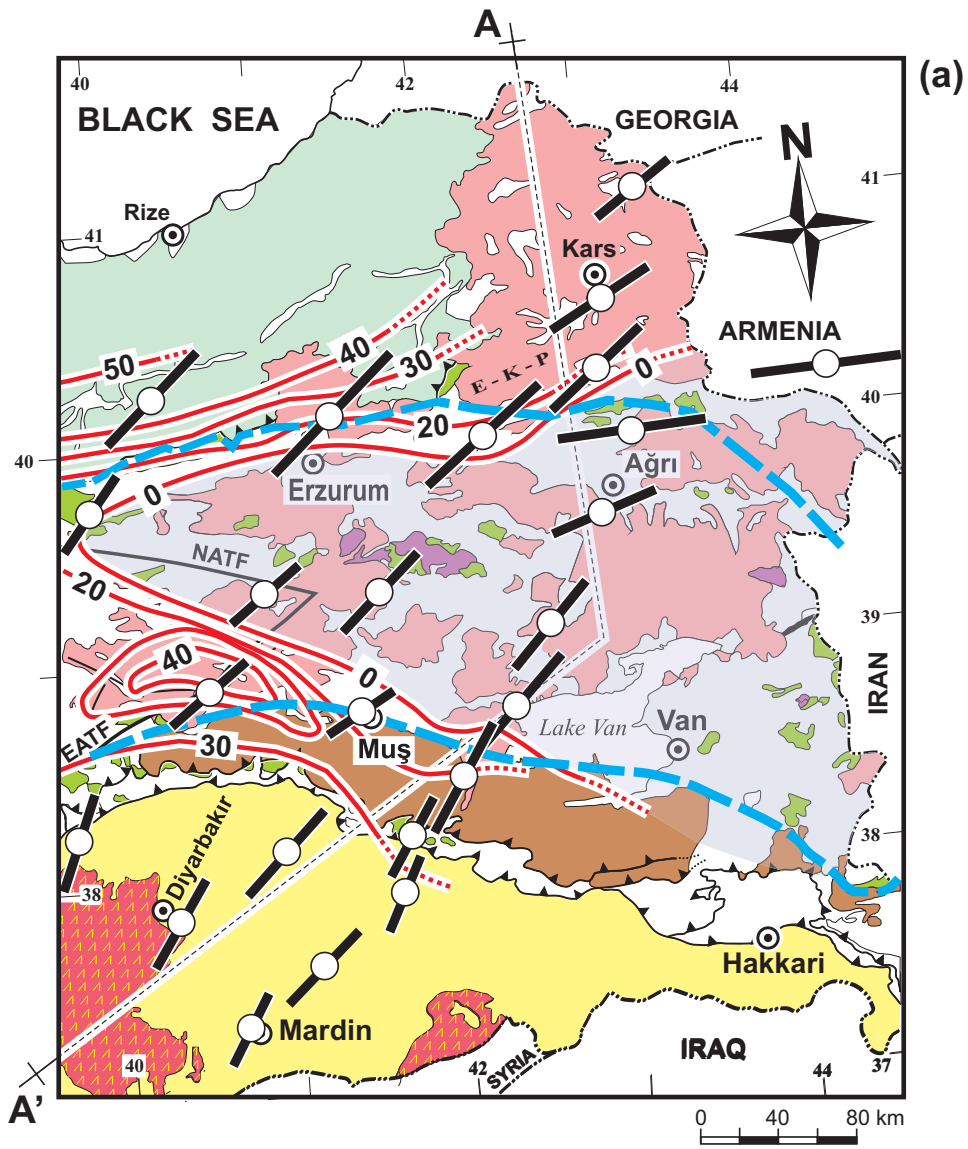


Figure: 3.

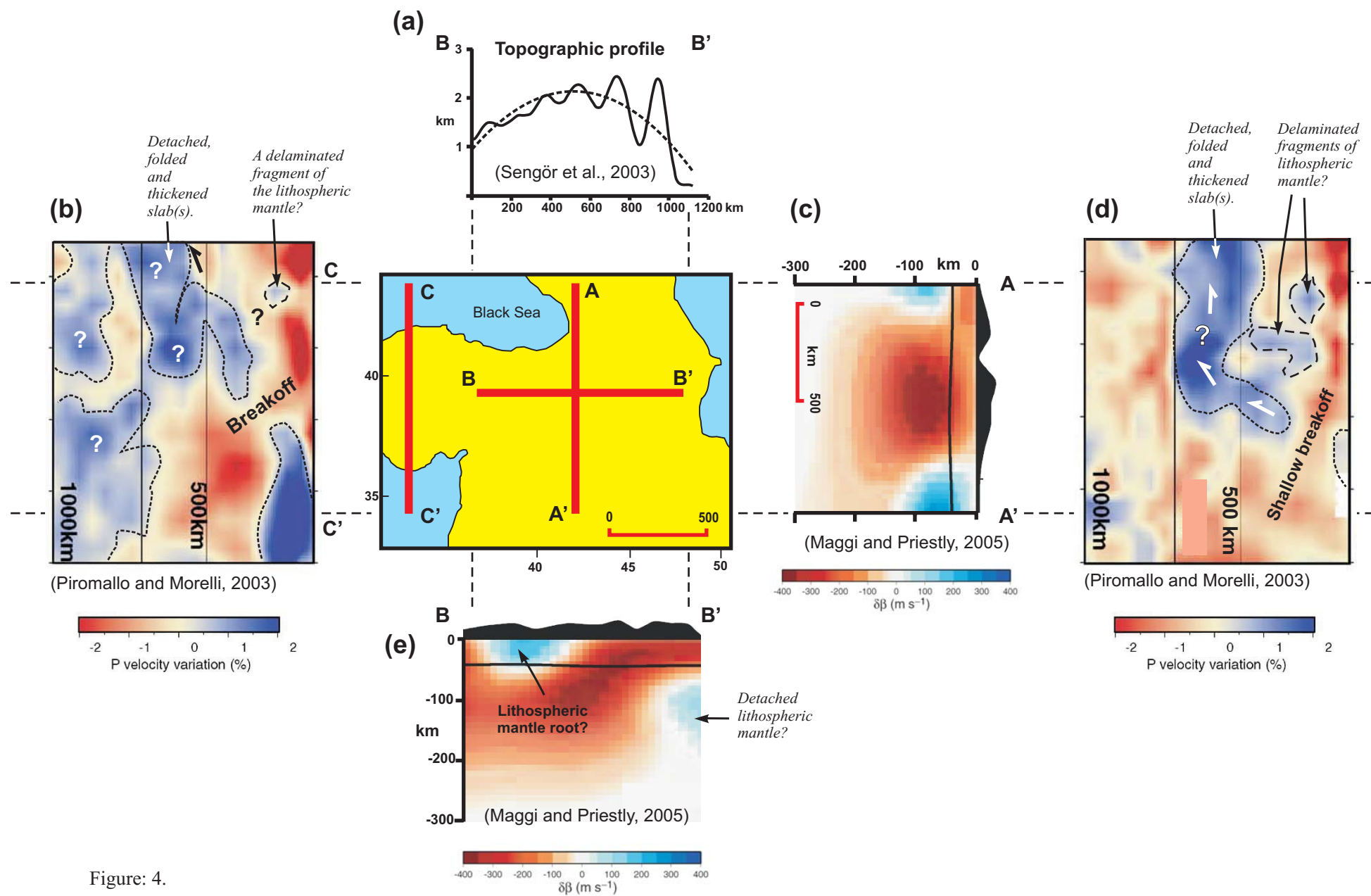


Figure: 4.

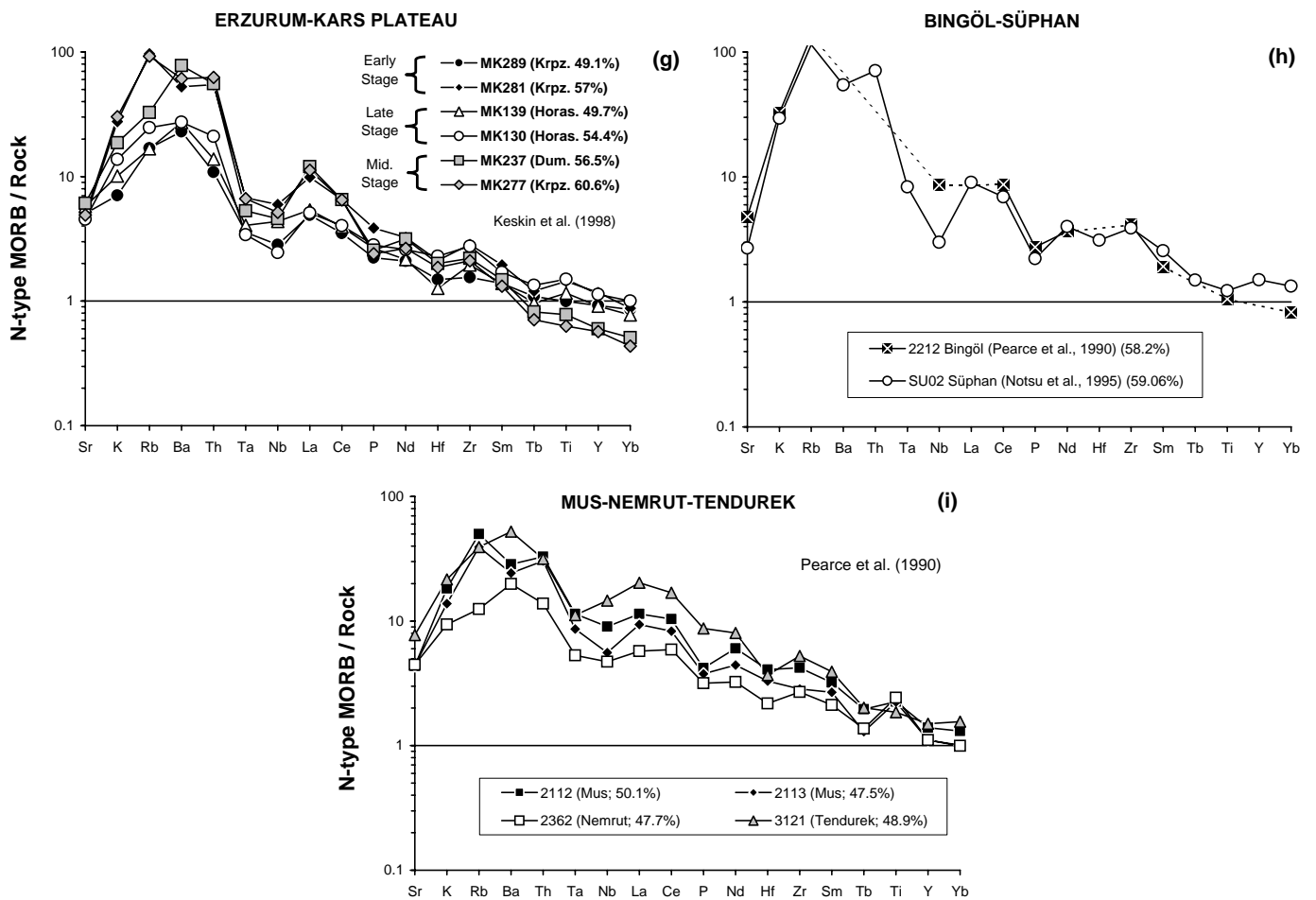
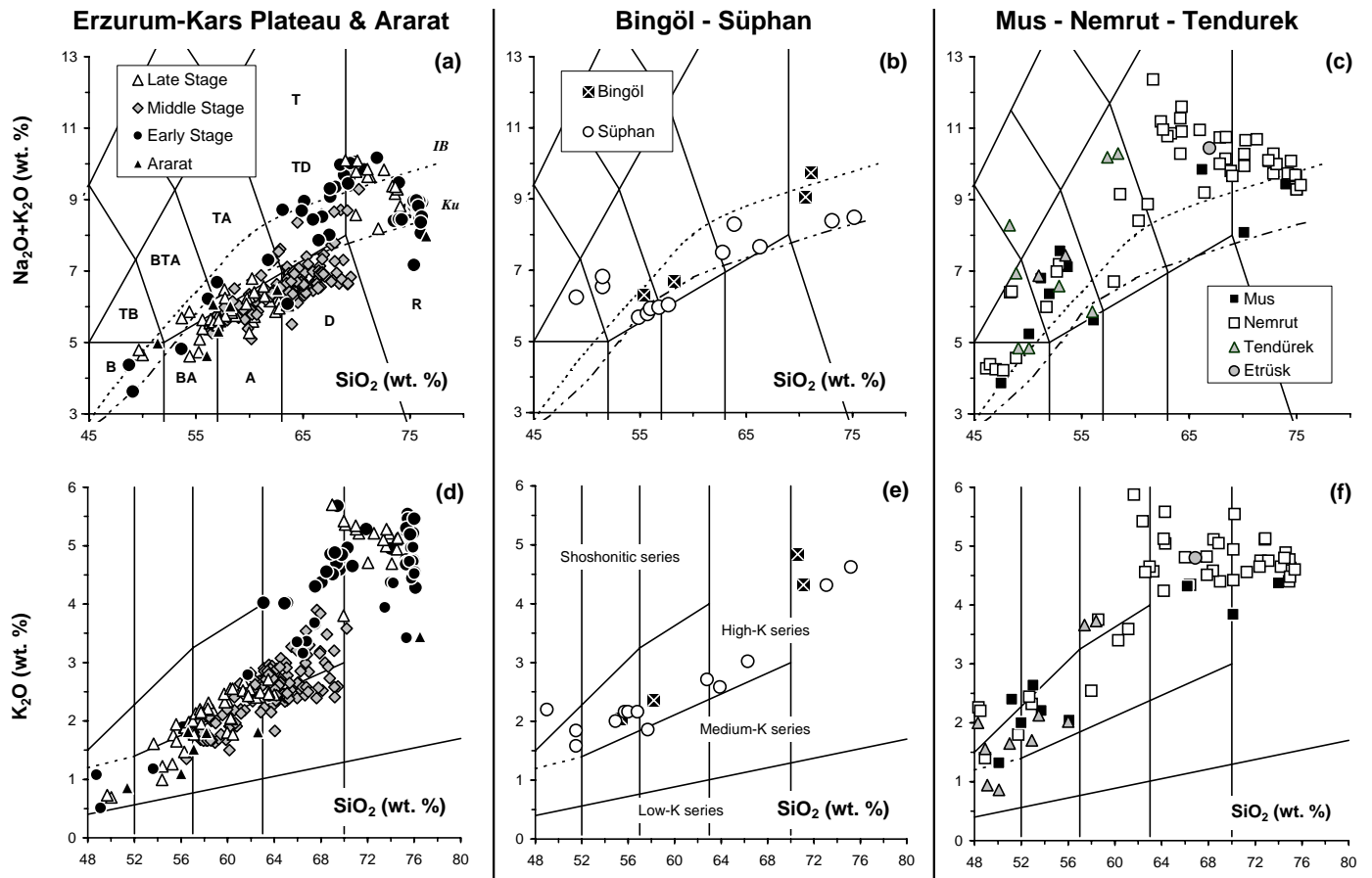


Figure 5.

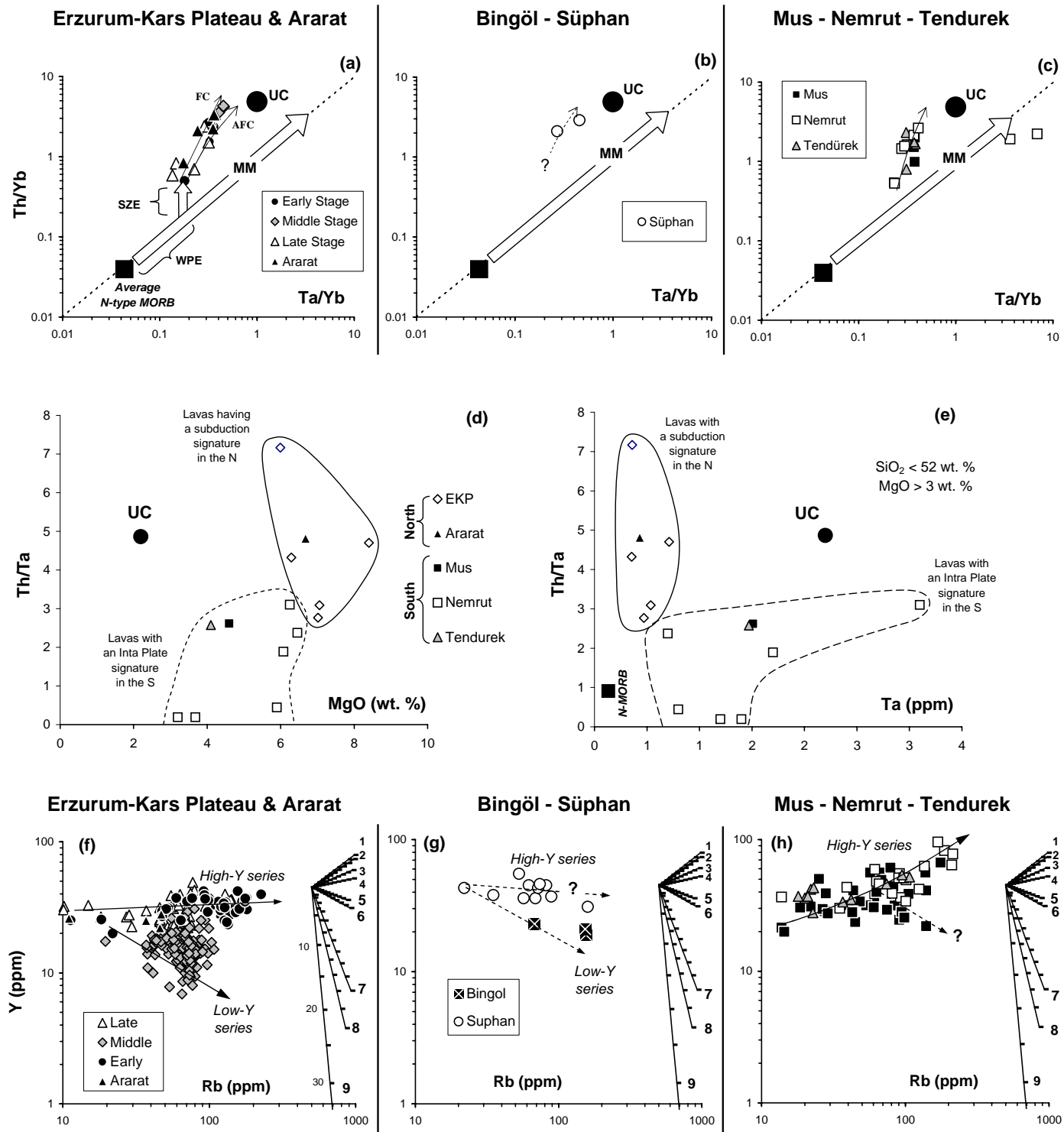
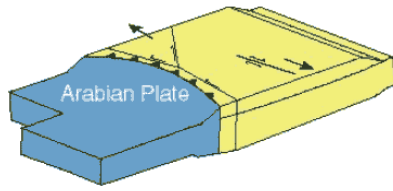
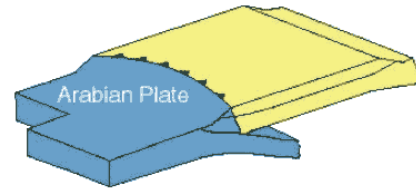


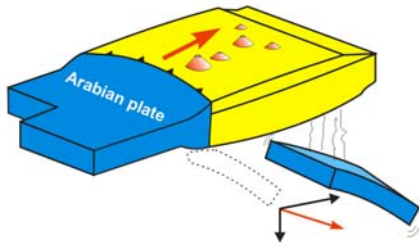
Figure 6.



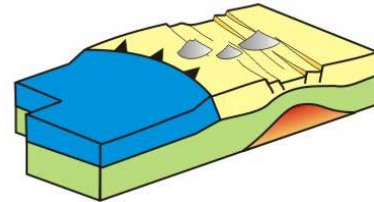
Model 1: The tectonic escape of micro-plates to the east and west (*McKenzie, 1972*).



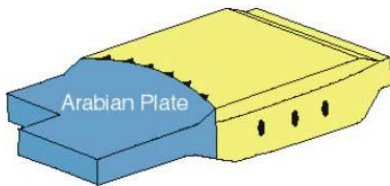
Model 2: Renewed continental, subduction of the Arabian plate beneath Eastern Anatolia (*Rotstein & Kafka, 1982*).



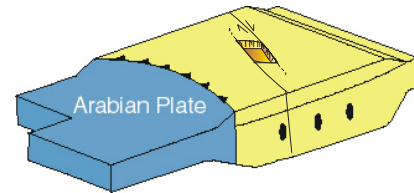
Model 3: Detachment and northward movement of a subducting slab beneath Eastern Anatolia (*Innocenti et al., 1982a,b*).



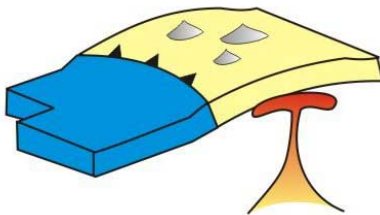
Model 4: Lithosphere extension following collision. Rifting along E-W oriented Late Miocene-Pliocene basins (*Tokel, 1985*) possibly accompanied by decompression melting of "normal asthenosphere" due to extension (*McKenzie & Bickle, 1988*).



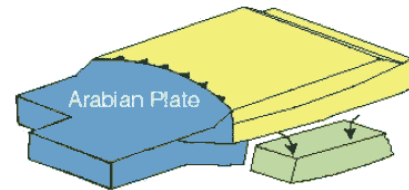
Model 5: Continental collision and subsequent thickening of the Anatolian crust/lithosphere (*Dewey et al., 1986*).



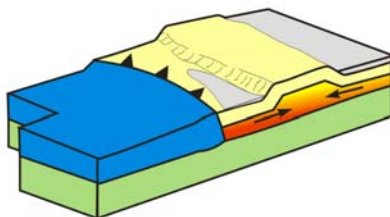
Model 6: Localized extension associated with pull-apart basins in strike-slip systems (*Dewey et al., 1986; Pearce et al., 1990; Keskin et al., 1998*).



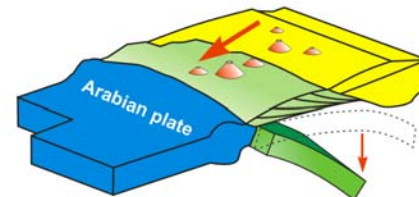
Model 7: Mantle plume impacts following collision (tested by *Pearce et al., 1990*; proposed as a model by *Ershov and Nikishin, 2004*).



Model 8: Delamination of mantle lithosphere beneath the region (proposed by *Pearce et al., 1990*; refined by *Keskin et al., 1998*).

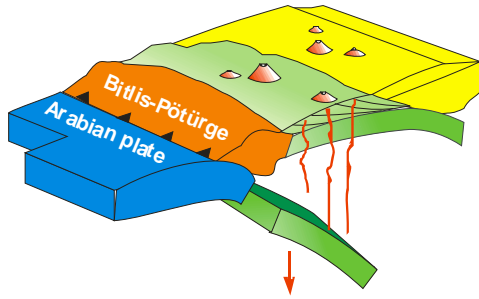


Model 9: Inflow of lower crust driven by the isostatic response to denudation and sedimentation in surrounding areas (*Mitchell & Westaway, 1999*).



Model 10: Slab-steepening and breakoff beneath a subduction-accretion complex (proposed by *Sengor et al., 2003*; supported by *Keskin, 2003*).

Figure: 7.

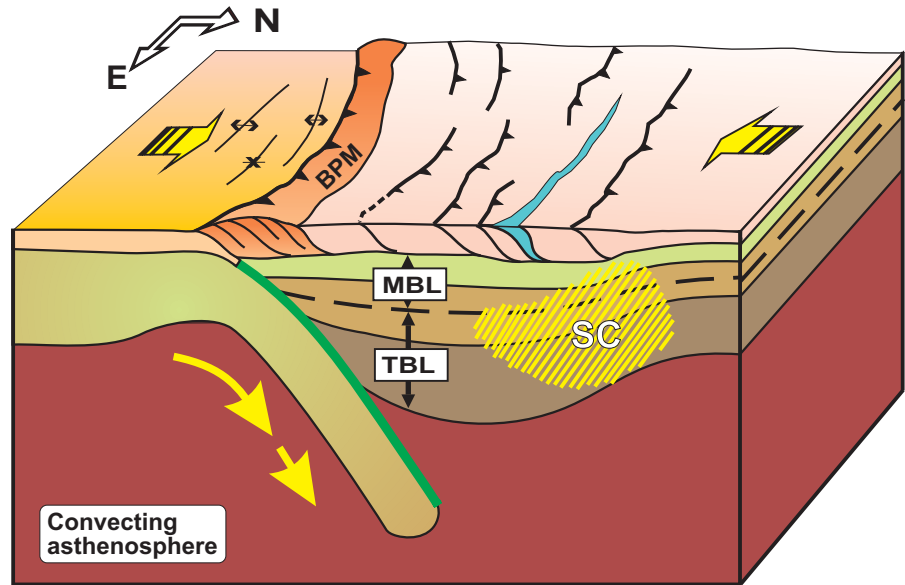
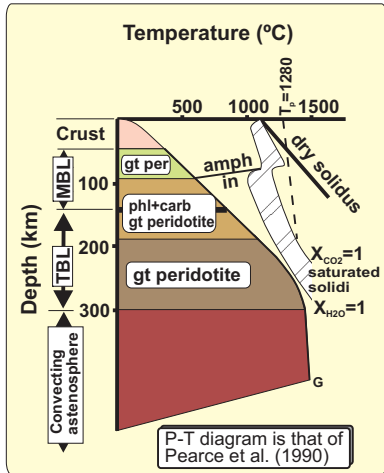


Modified slab-breakoff model involving two slabs subducting to the north (*Barazangi et al., 2006*).

Figure: 7.

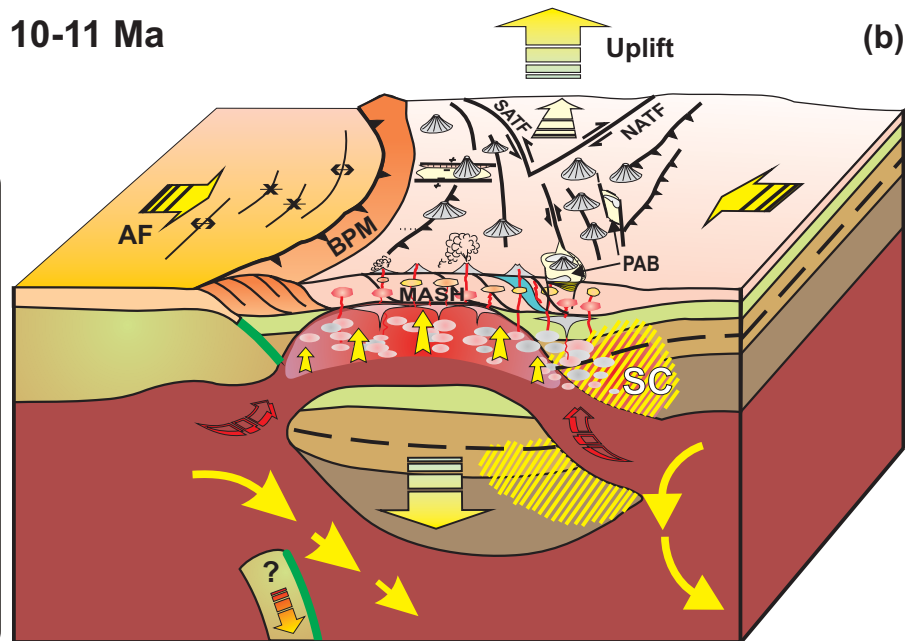
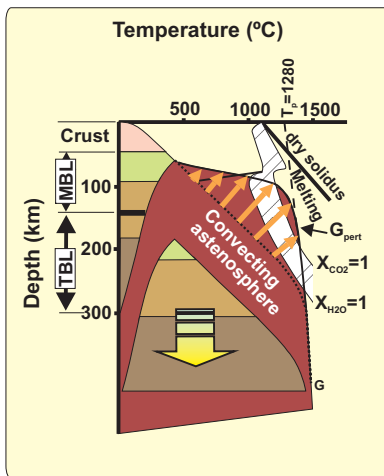
# Late Eocene

(a)



# 10-11 Ma

(b)



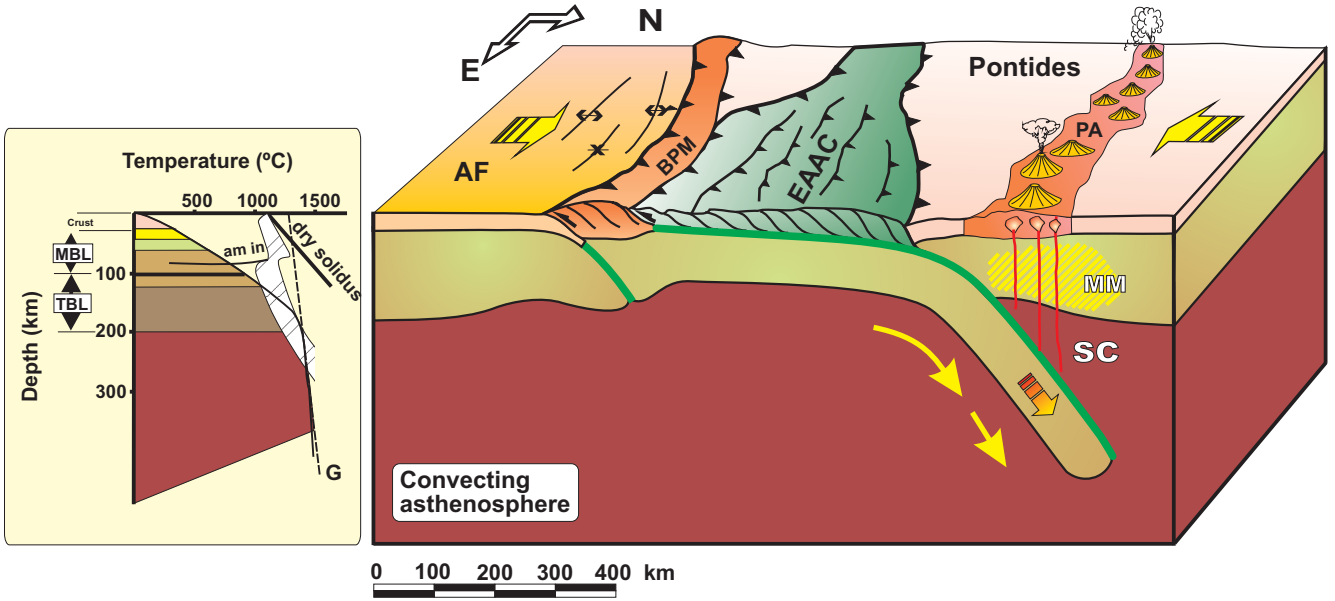
## EXPLANATIONS

- |   |  |  |
|---|--|--|
| Continental crust of Arabian foreland           | Garnet peridotite  | Volcanoes  |
| Thickened continental crust of Eastern Anatolia | Metasomatised lithosphere Phlogopite, carbonate, garnet peridotite                               | Thrusts  |
| Cretaceous -Eocene ophiolitic suture            | LIL element enriched lithosphere due to metasomatism created by Cretaceous Eocene arc volcanism. | Strike-slip faults                                   |
| Lithospheric mantle of the Arabian continent    | Partial melting zone in metasomatised sub-continental lithosphere and asthenosphere              | Crustal magma chambers (Red: deep, yellow: shallow). |
| Oceanic crust                                   | Garnet peridotite  |  |
|   | Convecting asthenosphere   |  |

Figure: 8.

# Late Oligocene-Early Miocene

(a)



10-11 Ma

Uplift

(b)

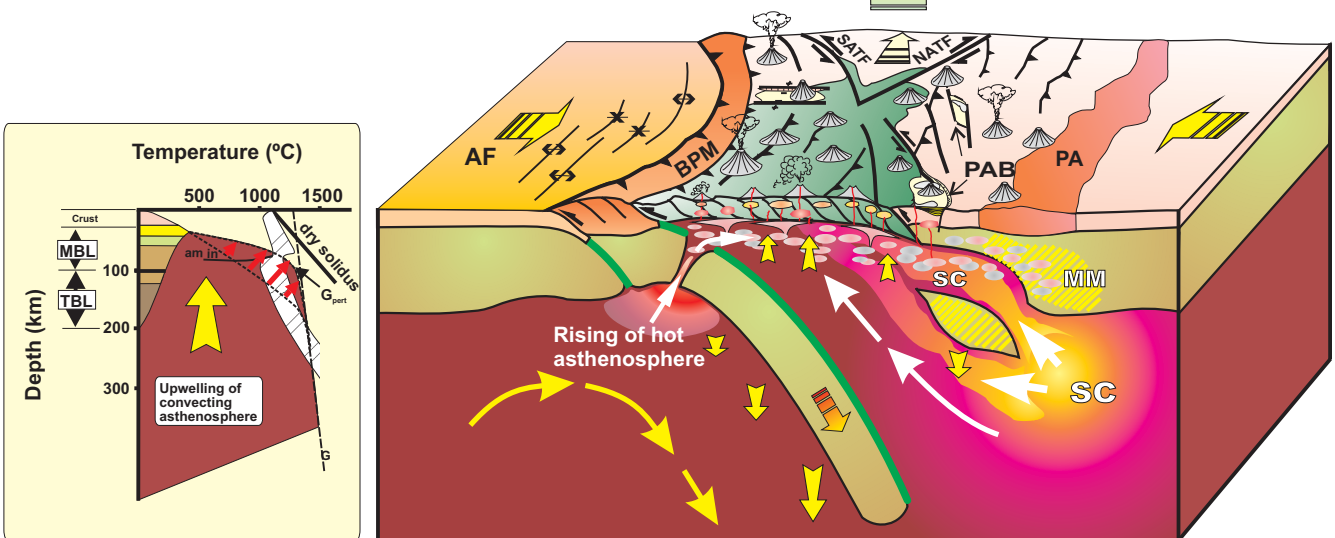


Figure: 9.

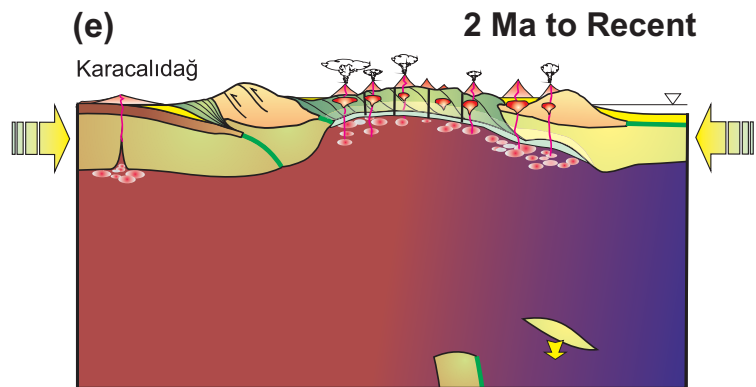
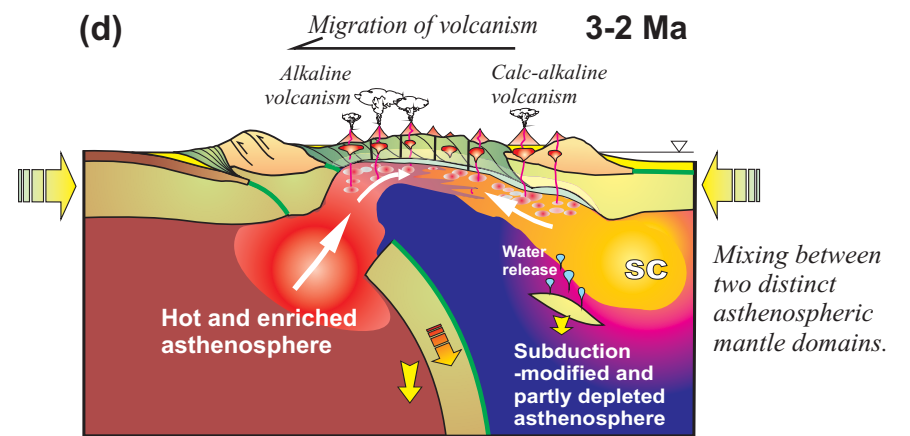
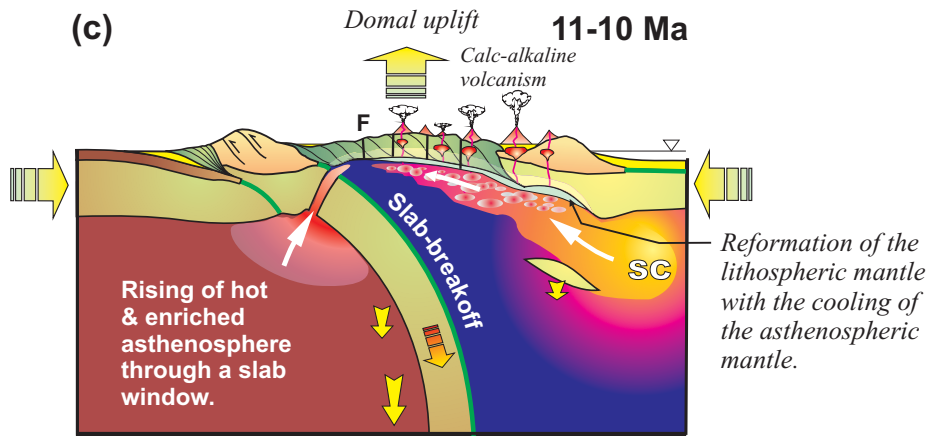
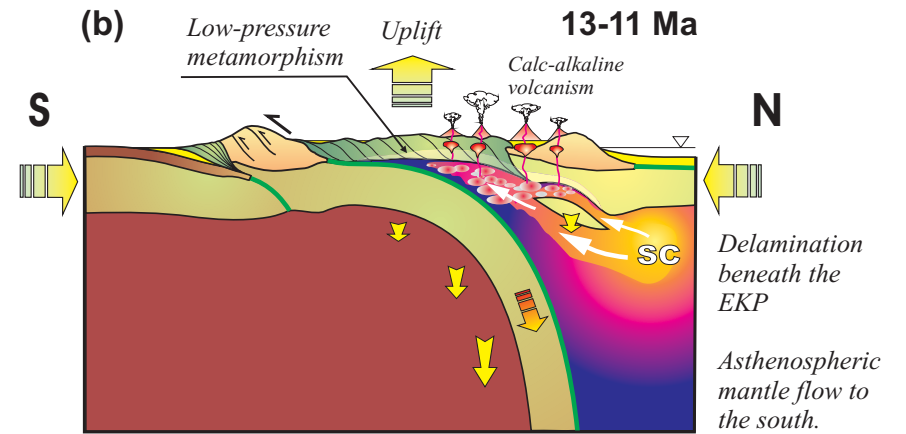
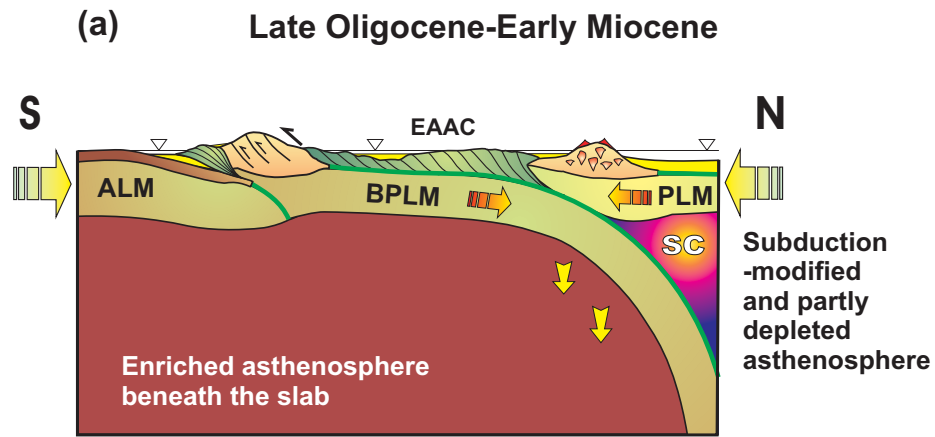


Figure: 10

Table: 1

Area	Author	Stage	Sample	SiO <sub>2</sub>	TiO <sub>2</sub>	Al <sub>2</sub> O <sub>3</sub>	Fe <sub>2</sub> O <sub>3</sub>	MnO	MgO	CaO	Na <sub>2</sub> O	K <sub>2</sub> O	P <sub>2</sub> O <sub>5</sub>	L.O.I.	Total	Sc	V	Cr	Co	Ni	Cu	Zn	Ga	Rb	Sr	Y	Zr	Nb	Ba	
NORTH	EKP	Keskin	Early	MK289	49.09	1.26	16.92	10.56	0.15	7.02	10.13	3.11	0.51	0.26	1.47	99.01	28	163	261	47	150	96	104	20	11	455	25	115	8	143
	EKP	Keskin	Early	MK281	56.99	1.83	16.12	8.81	0.11	2.23	5.73	4.68	2.00	0.45	0.97	99.04	22	183	3	11	3	20	83	18	52	417	31	213	14	335
	EKP	Keskin	Middle	MK237	56.47	0.99	18.43	6.63	0.10	4.16	7.33	3.91	1.35	0.30	1.40	99.66	18	132	51	20	22	16	69	20	20	564	17	158	12	495
	EKP	Keskin	Middle	MK277	60.58	0.80	15.85	5.22	0.08	4.08	6.10	4.11	2.18	0.28	0.84	99.28	11	99	116	21	95	32	55	20	62	489	16	159	14	450
	EKP	Pearce	Late	3011	46.00	2.42	16.90	13.90	0.21	5.81	8.49	4.04	0.61	0.58	1.13	100.09		120	22		43		89		5	518		275	10	
	EKP	Keskin	Late	MK144	48.76	1.34	15.18	9.10	0.33	8.40	11.40	3.29	1.08	0.54	2.47	99.41	24	201	264	62	212	66	85	16	18	867	26	119	15	533
	EKP	Keskin	Late	MK139	49.67	1.47	17.03	9.77	0.15	7.06	9.78	4.06	0.73	0.31	0.30	100.03	29	183	162	39	85	41	75	22	9	507	25	147	11	461
	EKP	Keskin	Late	MK130	54.36	1.90	15.81	9.71	0.18	4.56	7.90	4.87	0.99	0.33	0.14	100.61	26	163	11	35	32	20	75	19	15	415	33	214	7	175
	EKP	Pearce	Late	PL2/21	64.40	0.99	17.12	4.64	0.03	0.26	4.66	4.60	1.94	0.35	1.17	100.16		126	8		6	26	73		50	554	22	225	13	701
	Mt. Ararat	Pearce		3132	51.40	2.08	17.54	9.88	0.15	6.68	8.42	4.12	0.86	0.33	0.17	101.63	28	213	298	32	100	43	89		11	531	26	187	10	221
Mt. Ararat	Pearce		3031	56.60	1.35	16.94	7.60	0.11	3.16	6.08	4.25	1.82	0.31	0.82	99.07	16	191	81	19	25	26	84		47	463	28	229	12	461	
Mt. Ararat	Pearce		3041	58.20	0.97	17.50	6.37	0.09	4.08	6.57	4.22	1.80	0.30	0.29	100.39		111	103		67		69		46	532	22	203	13		
Mt. Ararat	Pearce		3131	62.60	0.79	18.00	5.40	0.09	1.42	4.59	4.67	1.81	0.29	0.47	100.13		56	5		10		73		41	379		207	13		
MIDDLE	Bingöl	Pearce		2212	58.20	1.34	17.90	7.69	0.17	1.37	5.94	4.32	2.36	0.32	2.12	101.73		108	24		33	73		75	433		306	20		
	Bingöl	Pearce		2214	70.60	0.36	15.30	2.30	0.04	0.24	1.56	4.22	4.84	0.11	1.89	101.46		13	2		6	41		155	155	19	307	23		
	Süphan	Pearce		2521	62.80	1.01	16.10	6.38	0.11	1.45	3.94	4.79	2.71	0.32	1.05	100.65		46	3		6	76		82	207	45	364	13		
	Süphan	Pearce		2531	63.90	0.87	17.30	5.90	0.11	1.33	3.80	5.71	2.58	0.24	0.46	102.20		42	6		10	70		80	200		338	10	392	
SOUTH	Muş	Buk-Tem		4	45.65	2.72	17.46	14.11	0.19	4.58	9.06	4.58	1.16	0.72		100.23	8	115	30	37	35		81	23	19	1082	30	339	22	155
	Muş	Pearce		2112	50.10	2.86	15.56	12.60	0.20	4.60	8.00	3.92	1.32	0.49	1.24	100.89	26	253	99	30	23	40	127		28	393	39	313	21	180
	Muş	Pearce		2111	53.70	1.45	18.20	9.53	0.18	2.21	6.38	4.90	2.21	0.44	1.68	100.88		67	12		21	100		63	422	40	430	28	184	
	Muş	Buk-Tem		1	56.35	1.55	17.54	7.94	0.12	3.36	6.28	4.40	1.95	0.52		100.01	15	133	8	26	19		100	25	54	492	32	30	35	335
	Muş	Buk-Tem		21	61.47	1.33	17.24	6.31	0.04	0.81	3.75	5.33	3.27	0.37		99.92	9	99	10	18	10		77	28	140	340	41	517	36	436
	Muş	Buk-Tem		16	63.01	0.81	16.65	5.08	0.09	2.42	5.09	3.80	2.78	0.25		99.98	9	77	24	29	18		41	19	95	399	28	269	24	693
	Muş	Pearce		2141	66.20	0.50	18.00	2.54	0.00	0.00	2.01	5.52	4.32	0.19	1.11	100.39					11		83		138	242	56	647	39	409
	Nemrut	Pearce		2362	47.70	3.08	16.66	14.10	0.20	6.46	9.48	3.54	0.68	0.37	-0.02	102.25	24	250	97	44	44	40	116		7	401	31	200	11	125
	Nemrut	Özdemir		Yoz 81	51.75	2.69	15.98	12.47	0.18	3.20	7.01	4.19	1.80	0.53		99.80	22	203		26		6	75	24	39	361	43	269	18	387
	Nemrut	Özdemir		Z-12	58.58	1.25	16.87	7.71	0.18	1.72	4.06	5.40	3.75	0.44	0.10	100.06	9	41		11		6	74	26	91	340	55	425	29	566
	Nemrut	Pearce		2022	64.30	0.55	15.70	5.54	0.19	0.26	1.41	6.02	5.58	0.10	0.42	100.07				1	9		103		93	19	466	33	245	
	Nemrut	Pearce		2421	66.00	0.42	16.20	4.35	0.12	0.00	1.20	6.14	4.81	0.07	0.37	99.68				8			53		98	94	51	531	34	
	Nemrut	Özdemir		Z-11	68.45	0.49	11.88	7.53	0.21	0.03	0.53	5.64	5.11	0.01	0.10	99.98	8			1		3	175	37	211	2	64		68	
	Nemrut	Özdemir		Cu-11	70.15	0.38	10.07	6.72	0.17	0.02	0.37	5.52	4.42	0.02	1.70	99.54	1			1		13	15	37	249	2	150		74	8
	Tendürek	Pearce		3121	48.90	2.35	17.00	11.70	0.20	4.10	6.53	5.38	1.56	1.02	0.24	98.98		106			12		114		22	695	42	389	34	329
	Tendürek	Sen		31	51.00	1.87	17.14	11.20	0.19	4.10	7.35	5.22	1.65		0.08	99.80									23	504	28	246	26	455
Tendürek	Sen		28	53.50	1.52	17.20	9.96	0.19	2.88	6.24	5.31	2.13		0.33	99.26									37	525	34	342	33	546	
Tendürek	Pearce		3111	58.40	1.24	18.10	5.98	0.14	1.34	3.56	6.56	3.73	0.42	0.39	99.86		36	11		7		114		95	286	54	475	42	538	

Table: 1 (continued).

Area	Author	Sample	La	Ce	Pr	Nd	Sm	Eu	Gd	Tb	Dy	Ho	Er	Tm	Yb	Lu	Hf	Ta	Pb	Th	U	$^{87}\text{Sr}/^{86}\text{Sr}_{(i)}$	$^{143}\text{Nd}/^{144}\text{Nd}_{(i)}$	$^{206}\text{Pb}/^{204}\text{Pb}_{(i)}$	$^{207}\text{Pb}/^{204}\text{Pb}_{(i)}$	$^{208}\text{Pb}/^{204}\text{Pb}_{(i)}$	$\delta^{18}\text{O}$	
NORTH	EKP	Keskin	MK289	12.3	26.3	3.4	15.3	3.64	1.34	3.8	0.73	4.32	0.88	2.62	0.40	2.61	0.41	3.1	0.47	21.2	1.30	0.41	0.703904	0.512847	17.663	15.553	37.493	
	EKP	Keskin	MK281	24.7	48.9	5.9	23.6	5.12	1.79	5.4	0.81	4.90	1.03	2.92	0.44	2.67	0.41	4.3	0.89	9.0	6.55	1.90	0.703931	0.512898	18.734	15.603	38.748	
	EKP	Keskin	MK237	30.1	48.9	5.8	23.0	3.90	1.28	3.6	0.55	3.06	0.58	1.62	0.24	1.55	0.25	4.1	0.70	12.6	6.67	1.11						
	EKP	Keskin	MK277	28.1	48.6	5.3	19.3	3.48	0.99	3.0	0.47	2.50	0.51	1.48	0.24	1.33	0.21	3.8	0.88	11.5	7.50	2.06	0.704322	0.512781	18.682	15.605	38.721	7.2
	EKP	Pearce	3011		46.4		27.5	6.17	2.05	5.6		5.99		3.50		3.29							0.703800					
	EKP	Keskin	MK144	30.6	68.9	8.3	33.7	6.14	1.74	5.7	0.71	4.05	0.83	2.20	0.32	2.18	0.34	2.8	0.71	5.6	3.34	1.03	0.704570	0.512791	19.022	15.664	39.053	
	EKP	Keskin	MK139	13.5	29.6	3.8	15.8	3.64	1.33	4.1	0.65	4.14	0.80	2.46	0.35	2.37	0.35	2.6	0.53	2.6	1.65	0.70	0.703705	0.512931	18.933	15.667	39.031	
	EKP	Keskin	MK130	12.8	30.2	4.0	18.9	4.48	1.56	4.9	0.90	5.15	1.04	3.08	0.47	3.05	0.48	4.7	0.45	5.1	2.52	0.67	0.703390	0.512930	18.939	15.623	38.895	
	EKP	Pearce	PL2/21																	8.0			0.704180					
	Mt. Ararat	Pearce	3132	18.9	52.7		26.6	5.17	1.63		0.69		0.83			2.46	0.41	4.2	0.43	3.0	2.07	0.30	0.703890					
Mt. Ararat	Pearce	3031	26.9	67.8		29.1	5.50	1.62		0.53					2.74	0.46	5.4	0.67	10.0	5.78	1.99	0.704170						
Mt. Ararat	Pearce	3041	29.6	64.1		25.8	4.41	1.36		0.51					1.88	0.34	4.1	0.68	8.0	6.29	2.20	0.704160						
Mt. Ararat	Pearce	3131		47.3		20.6	3.96	1.22	3.5		3.58		1.96		1.95							0.704410						
MIDDLE	Bingöl	Pearce	2212		65.1		26.7	5.04	1.43	4.3		4.53		2.55	2.53							0.704730	0.512745					
	Bingöl	Pearce	2214																	21.0	22.00		0.705060					
	Süphan	Pearce	2521		65.1		31.0	6.77	1.98	7.2		7.69		4.63	4.40					12.0	10.00		0.705050	0.512842				
	Süphan	Pearce	2531		86.3		33.1	5.57	1.33	6.1		6.67		4.03	3.97								0.704660					
SOUTH	Muş	Buk-Tem	4	25.0	50.0		31.6	6.60	1.90		0.78				2.80	0.50	5.4			2.20	14.00	0.704660	0.512860					
	Muş	Pearce	2112	28.6	77.7		44.1	8.45	2.40		1.31		1.57		4.00	0.61	8.4	1.51	6.0	3.95	0.73	0.704320						
	Muş	Pearce	2111	35.4	90.7		45.8	8.92	2.33		1.07				4.41	0.61	8.8	1.67	7.0	8.81	1.71	0.704430	0.512793					
	Muş	Buk-Tem	1	44.0	69.0		29.2	5.80	1.80		0.00				3.00	0.70	6.2			7.50	6.00	0.704160	0.512800					
	Muş	Buk-Tem	21	47.0	83.0		35.8	6.90	1.50		0.97				3.40	0.60	9.4			19.00	17.00	0.704820	0.512760					
	Muş	Buk-Tem	16	41.0	64.0		26.0	4.70	1.30		0.93				2.40	0.50	5.9			12.00	15.00	0.705000	0.512710					
	Muş	Pearce	2141	41.9	113.1		57.1	11.06	1.63		1.16				4.47	0.80	10.7	3.03	20.0	17.28	7.68	0.705440						
	Nemrut	Pearce	2362	14.4	44.4		23.6	5.56	4.41		0.92		1.28		3.04	0.45	4.5	0.70		1.66	0.23	0.703570						
	Nemrut	Özdemir	Yoz 81	31.3	64.1	8.4	35.3	7.60	2.53	7.5	1.29	7.33	1.64	4.15	0.60	4.04	0.60	6.7	1.20	1.3	6.30	1.30						
	Nemrut	Özdemir	Z-12	48.1	90.8	11.3	47.5	10.10	2.80	9.0	1.58	9.27	1.93	5.56	0.87	5.94	0.89	9.9	2.20	2.3	12.70	3.00						
	Nemrut	Pearce	2022	43.3	100.9		47.3	10.33	5.99		1.09				5.44	0.71	12.2	1.70		8.97	1.84	0.706080						
	Nemrut	Pearce	2421																	11.0	12.00		0.705050					
	Nemrut	Özdemir	Z-11	62.0	178.5	16.6	63.9	14.80	1.03	13.0	2.47	15.67	3.36	10.67	1.74	12.14	1.99	25.6	4.70	23.3	25.00	3.70						
	Nemrut	Özdemir	Cu-11	109.6	239.8	27.3	111.7	23.20	1.53	22.5	4.21	25.27	4.88	15.44	2.35	15.03	2.02	32.4	4.80	13.0	34.20	10.10						
	Tendürek	Pearce	3121	50.6	126.3		58.5	10.34	2.88		1.35				4.75	0.76	7.6	1.47	12.0	3.79	0.96	0.705630						
	Tendürek	Sen	31	44.2	90.2	10.5	37.7	7.37	2.54	9.1		6.06	1.10	3.11	0.48	2.94	0.49	5.0	1.10	11.3	5.13	1.63	0.705743	0.512676				
	Tendürek	Sen	28	57.0	115.0	13.2	46.6	8.92	3.08	11.5		7.74	1.40	3.86	0.62	3.91	0.61	7.0	1.51	15.4	6.45	1.95	0.705889	0.512676				
Tendürek	Pearce	3111	58.6	128.4		50.9	8.53	2.41		1.34				5.28	0.93	9.8	1.63	17.0	12.20	3.73	0.705340	0.512816						